International Journal of Heat and Fluid Flow 30 (2009) 617–636

Contents lists available at ScienceDirect

International Journal of Heat and Fluid Flow

journal homepage: www.elsevier.com/locate/ijhff

Separation-induced boundary layer transition: Modeling with a non-linear eddy-viscosity model coupled with the laminar kinetic energy equation

Z. Vlahostergios, K. Yakinthos *, A. Goulas

Laboratory of Fluid Mechanics and Turbomachinery, Department of Mechanical Engineering, Aristotle University of Thessaloniki, Karamanli str., Thessaloniki 54124, Greece

ARTICLE INFO

Article history:
Received 23 September 2008
Received in revised form 18 February 2009
Accepted 19 February 2009
Available online 14 April 2009

Keywords:
Separation-induced transition
Laminar kinetic energy
Non-linear eddy-viscosity model

ABSTRACT

We present an effort to model the separation-induced transition on a flat plate with a semi-circular leading edge, using a cubic non-linear eddy-viscosity model combined with the laminar kinetic energy. A non-linear model, compared to a linear one, has the advantage to resolve the anisotropic behavior of the Reynolds-stresses in the near-wall region and it provides a more accurate expression for the generation of turbulence in the transport equation of the turbulence kinetic energy. Although in its original formulation the model is not able to accurately predict the separation-induced transition, the inclusion of the laminar kinetic energy increases its accuracy. The adoption of the laminar kinetic energy by the non-linear model is presented in detail, together with some additional modifications required for the adaption of the laminar kinetic energy into the basic concepts of the non-linear eddy-viscosity model. The computational results using the proposed combined model are shown together with the ones obtained using an isotropic linear eddy-viscosity model, which adopts also the laminar kinetic energy concept and in comparison with the existing experimental data.

1. Introduction

It is well known that the transition of a boundary layer, from the laminar regime to the turbulent one, is a complex and stochastic phenomenon. The physics of a transitional flow has been widely investigated, but in most cases for simplified situations by trying to isolate the various parameters affecting transition. The most interesting fluid mechanics applications, which involve boundary layer transition, are related to the flow development on airfoils, wings and turbomachinery blade surfaces. Typically, during the operation of such devices, transition occurs due to three essential mechanisms: natural transition, which is the most rare case, bypass transition, which is closely related to the freestream turbulence intensity and transition due to boundary layer separation. The latter is often occurring at some distance downstream of the leading edge of an airfoil or a turbine blade. In the stagnation point region, the boundary layer starts to develop as a laminar one with a high level of stability due to the surface curvature, which cause the flow to accelerate. The instability of the boundary layer starts to appear when the surface curvature diminishes and the favorable pressure gradient becomes an adverse pressure gradient. Under certain freestream conditions, i.e. low freestream velocity or turbulence intensity, the boundary layer separates and a recirculation zone is formed on the surface. In turn, the laminar boundary layer enters to the transitional zone before becoming turbulent. A series of well documented experiments showed that the size of the recirculation zone is greatly affected by the freestream conditions. Thus, depending on the level of freestream turbulence and the magnitude of freestream velocity, larger and thicker or smaller and thinner recirculation zones are formed and by consequence, rapid or slow transition procedure is observed, respectively. The importance of the transition mechanism is very high, especially in the design of airfoils and wings in the field of aeronautics and in the design of the turbomachine blades. The aerodynamicists need to accurately predict the transition-onset and duration in order to design airfoils which operate with a minimum danger to stall under high angle of attack or reduced speed of flight and the turbomachinery engineers need to accurately predict the transition-onset and duration, since it can affect the aerodynamic loading of the blades and the heat transfer mechanism between the hot fluid and the cold blade.

From the previous analysis it is clearly evident that there is a need for accurate and robust prediction methods for the transition-onset and duration. These methods should encounter all the primary and secondary parameters that can affect transition (freestream velocity and turbulence, surface curvature and pressure gradient, etc.) and should provide accurate results obtained with the minimum amount of empiricism and the maximum amount of well-founded theory regarding boundary layer transition. Towards this direction, the most accurate prediction method is

* Corresponding author. Tel.: +30 2310996411; fax: +30 231096002.
E-mail address: kyros@eng.auth.gr (K. Yakinthos).

0142-727X/$ - see front matter © 2009 Elsevier Inc. All rights reserved.
doi:10.1016/j.ijheatfluidflow.2009.02.004

Nomenclature

D_T	near-wall dissipation for turbulent kinetic energy
D_L	near-wall dissipation for laminar kinetic energy
k_T	turbulent kinetic energy ($= k_{T,l} + k_{T,s}$)
$k_{T,l}$	large-scale of turb. kinetic energy
$k_{T,s}$	small-scale of turb. kinetic energy
k_L	laminar kinetic energy
k_{TOT}	total kinetic energy ($= k_{T,l} + k_{T,s} + k_L$)
P_L	production of lam. kinetic energy
P_T	production of turb. kinetic energy
S_{ij}	strain rate tensor [$= (\partial U_i/\partial x_j + \partial U_j/\partial x_i)$ for the Craft et al. Model (1996)] [$= 0.5(\partial U_i/\partial x_j + \partial U_j/\partial x_i)$ for the Walters and Leylek Model (2004)]
S	magnitude of mean strain rate tensor($= \sqrt{2S_{ij}S_{ij}}$)
Ω_{ij}	rotation rate tensor [$= (\partial U_i/\partial x_j - \partial U_j/\partial x_i)$ for the Craft et al. Model (1996)] [$= 0.5(\partial U_i/\partial x_j - \partial U_j/\partial x_i)$ for the Walters and Leylek Model (2004)]
Ω	magnitude of mean rotation tensor ($= \sqrt{2\Omega_{ij}\Omega_{ij}}$)
R	by-pass transition production term
R_{NAT}	natural transition production term
f_v	viscous damping function
f_{INT}	intermittency damping function
$f_{\tau,l}$	time scale damping function for large-scale turbulent viscocity
$f_{\tau,s}$	time scale damping function for small-scale turbulent viscocity
U_0	freestream velocity
U_{max}	maximum velocity (when the boundary layer is separated)

Greek symbols

ε	turbulence dissipation rate
$\tilde{\varepsilon}$	isotropic dissipation rate
$\tilde{\varepsilon}_s$	isotropic small-scale dissipation rate
λ_T	turbulent length scale
λ_{eff}	effective length scale
ν_t	eddy-viscosity
$\nu_{T,s}$	small-scale eddy-viscosity
$\nu_{T,l}$	large-scale eddy-viscosity
ν_{TOT}	total eddy-viscosity ($= \nu_{T,l} + \nu_{T,s}$)
$\tau_{T,s}$	small-scale turbulent time scale
$\tau_{T,l}$	large-scale turbulent time scale
τ_m	mean flow time scale

the stability theory, which examines the development of small instabilities in a laminar flow field with the use of the Orr–Sommerfeld equation and its solutions based on the wavelengths of the small instabilities (Schlichting and Gersten, 2000). Despite of the inclusion of some assumptions in the development of this theoretical approach, its application has been found to be very difficult in complex flows, which involve boundary layer separation also, and due to this difficulty, the solution of the Orr–Sommerfeld equation is performed usually for cases with natural or by-pass transition. Besides that, there is a certain difficulty for an engineer to correlate the theoretical wavelength of a specific imposed instability with a practical characteristic length of a mechanical device.

An alternative and modern approach is the use of DNS but the computational cost, when it is applied in complex configurations, such as airfoils and turbine blades, is still high. Durbin and Xu (2007) presented computer simulations by applying the pertinent linear theory in order to have a picture of the transition beneath vortical structures. Recently, Schmid (2007) presented an approach for the first stages of the by-pass transition in the framework of the non-modal stability theory.

It is more than fifteen years that transition has been modeled with the use of the Reynolds Averaged Navier–Stokes equations. Especially, for the by-pass transition, since it is a stochastic phenomenon, it can be faced using the tools of statistical fluid mechanics, therefore, the use of properly designed transition models in the framework of RANS can be a feasible approach. Although this approach seems to be an "oxymoron" (one is trying to model a flow that starts as laminar with a set of equations for turbulent flow), the results presented so far, showed some good perspectives. The basic idea of the approach is focused on the use of eddy-viscosity or Reynolds-stress models in their low-Reynolds number formulations. The use of low-Re formulations has been found to be very helpful and at first, a good remedy for providing a practical solution to the "oxymoron" of the approach mentioned above. Savil (2002a,b) reported, in two very detailed articles regarding the attempts and the strategies in modeling by-pass transition, that the low-Re formulations of the eddy-viscosity models provided a limited success due to the damping effect, introduced by the damping functions, which forces the pre-transitional boundary layer to behave as pseudo-laminar. The success of by-pass transition modeling is limited due to the incapability of these models to present, inside the boundary layer, accurate predictions for the Reynolds-stresses (longitudinal and shear stresses) together with the turbulence kinetic energy distributions, in the pre-transitional, transitional and fully turbulent flow regime. Among the attempts to model by-pass transition, we focus on the work of Craft et al. (1997) who presented quite accurate results regarding both the velocity and turbulent quantities parameters with the use of a non-linear eddy-viscosity model, developed by the same group (Craft et al. 1996) together with a third transport equation for the stress invariant A_2, which is based on the anisotropic Reynolds-stress tensor a_{ij}. The stress invariant was included in order to ensure the Reynolds-stress anisotropic behavior close to the wall, an action, which can improve the boundary layer modeling in transitional flows (Savill, 2002a). We should also refer to the work of Wilcox (1991) who was the first to use the k–ω eddy-viscosity variant in a low-Reynolds formulation, by introducing damping functions also, in order to predict by-pass transition with good results. Of course, there are many other attempts regarding the use of pure eddy-viscosity models without any additional concepts, the reader can find a compilation of them in the work of Savill (2002a).

In parallel, during these fifteen years, a second alternative approach has also started to be applied and it was focused on the combination of the RANS equations, using a conventional turbulence model, with the intermittency factor concept. Cho and Chung (1992) were the first who presented an effort to combine the standard k–ε model with the intermittency factor in free shear layers, for the calculation of the eddy-viscosity. The intermittency factor acts as a damping function and, based on its transport equation, takes lower values or becomes zero in the laminar flow regime, while it takes values close to unity when the flow becomes turbulent. The eddy-viscosity is multiplied by this factor and by consequence, becomes zero or takes its full value depending on the flow regime, i.e. laminar, transitional or fully turbulent. Gostelow and Walker (1991) investigated experimentally the effect of the freestream turbulence levels together with the adverse pressure gradient on the boundary layer transition. They observed that un-

der high turbulence levels and adverse pressure gradients a pronounced subtransition was present. Additionally, they showed that a strong degree of similarity in intermittency distributions was observed. During the same time, the Vrije University Group (Hazarika and Hirsch 1992) presented detailed experimental data from measurements inside transitional boundary layers where the same observation regarding the similarity of the intermittency distributions was shown. Savill (1995) was the first to use an intermittency transport equation together with either the Savill–Launder–Younis Reynolds-Stress Transport model and a low-Re k–ε linear model in order to model the ERCOFTAC by-pass transitional flows with very good results. Regarding the application of the intermittency concept to separated flow transition, Vilmin et al. (2002) used an intermittency-conditioned modeling approach in order to model the wake-passing transition in turbomachinery by providing excellent numerical results for a variety of flow conditions on turbine and compressor blades. Parallel to the idea of the intermittency transport equation, Steelant and Dick (1996) presented an alternative procedure in order to model by-pass transition with the use of the "conditionally averaged" Navier–Stokes equations. Additionally, Suzen and Huang (1999) and Suzen et al. (2003) presented results for the by-pass boundary layer transition by using alternative formulations of the intermittency transport equation. The idea of using the intermittency transport equation together with an eddy-viscosity model seems to be promising but as already stated by Hadzic and Hanjalic (1999), it involves a degree of empiricism and this is clear to everyone who uses the intermittency models: these models use factors and parameters which are specifically calibrated depending on the new test case that must be modeled. Additionally, these models inevitably employ a correlation for the detection of the transition-onset point, which is different, depending on the transition mode.

To the authors' knowledge the majority of the efforts regarding transitional modeling have been focused on by-pass transition. A small number of contributions have been reported in the literature regarding the modeling of boundary layer separation-induced transition and probably this has to do with the major difficulties appearing during the modeling of such transitional flows. A typical difficulty is focused on the exact freestream conditions between experiment and modeling: since the recirculation zone is strongly affected by the freestream conditions (turbulence and velocity), a large effort must be made in order to match the exact freestream conditions of the experiment with the computational modeling. In many occasions, this leads to a number of trials in order to predict the correct turbulence decay and if a careful approach is not performed, the results can lead to wrong conclusions.

Palikaras et al. (2002, 2003) presented results for separation-induced transitional flows under uniform and positive shear, using eddy-viscosity models where they showed the incapability of such models to accurately predict the flow development. Vicedo et al. (2004) presented a detailed analysis for the combination of a k–ε model with an intermittency transport equation for the case of separation-induced boundary layer transition on a flat plate. Their results showed that the proposed intermittency transport model is able to provide far better results than typical modeling approaches, something which is very clearly shown on the distributions of the skin friction coefficient and of the displacement thickness for the examined separated transitional boundary layers, having either low or high freestream turbulence levels.

Reynolds-stress transport models, offering a more general framework to predict complex turbulent flows and transition, provide results whose dependence on the tuning of the model coefficients cannot be neglected. As reported by Savill (2002b), the combination of low-Reynolds number Reynolds-stress transport models together with an intermittency transport equation has also been proposed with success. Hadzic (1999) and Hadzic and Hanjalic (1999) presented accurate results regarding the separation-induced boundary layer transition using a modified low-Reynolds number Reynolds-stress model based on the one developed by Hanjalic and Jakirlic (1998). The model has been proved capable of capturing the total transition mechanism, from the pre-transitional flow regime up to the fully turbulent one, by having also the capability to provide the correct recirculation zone size and very accurate longitudinal Reynolds-stress distributions inside the boundary layer. Vlahostergios et al. (2007) presented results of similar quality with the use of a Reynolds-stress model developed by the University of Manchester group (Craft and Launder, 1996 and modified by Craft (1998)) in order to take into account the low-Reynolds number effects. The use of the Reynolds-stress model was made without any additional modification or any use of the intermittency factor but it should be noticed that based on our experience in the University of Thessaloniki group, the Reynolds-stress model computer algorithm needed a lot of additional stability measures in order to provide a robust and successful convergence.

So far we reported three major approaches for the transition modeling: the net use of an eddy-viscosity model in a low-Reynolds number formulation, the combination of an eddy-viscosity model, in most cases in a low-Reynolds number formulation, with an intermittency transport equation and the use of a Reynolds-stress model, again in a low-Reynolds number formulation. Unfortunately, each approach has its advantages and its disadvantages. Regarding the disadvantages, either the results are of low quality, especially for the prediction of the turbulent parameters (kinetic energy, Reynolds-stress) when a simple eddy-viscosity model is adopted, either they involve a lot of empiricism, when the intermittency factor is used, or finally they are not able to provide stable numerical convergence due to major instabilities within an iterative computation. All of these approaches assume that the flow starts as a turbulent one or having a very low turbulence intensity level.

Mayle and Schulz (1997) introduced a new theory for the by-pass transition involving the concept of the laminar kinetic energy. More specifically, they developed a transport equation for the laminar kinetic energy (k_l) and proposed models for the production and the dissipation terms in this equation. Under this idea, they stated that apart from the classic turbulence kinetic energy, there is the laminar kinetic energy also, that contributes to the transition mechanism inside a boundary layer and especially in the pre-transitional region. This energy takes higher values before transition and then starts to diminish as it gives its place to the turbulence kinetic energy. This idea has a practical application: one can solve an additional equation, through an eddy-viscosity approach, in order to have the distribution of the laminar kinetic energy. Then, the eddy-viscosity is appropriately computed using both the laminar and the turbulence kinetic energy. Walters and Leylek (2004) presented a first practical application of this concept where they modeled by-pass transition flows on a flat heated wall and on a turbine stator vane using a low-Reynolds number k–ε model. In order to closely connect the laminar kinetic energy with a simple linear eddy-viscosity model, they proceeded to some essential interventions: in the linear expression of the eddy-viscosity they introduced the total kinetic energy, which is the sum of the laminar and turbulent kinetic energy. Additionally, the turbulent kinetic energy appearing in the near-wall region was split into a small-scale and a large-scale turbulent energy. Both of them are computed using the appropriate small and large-scales of turbulence length scales. Walters and Leylek (2005) presented new results for wake-induced transition on a compressor-like flat plate using the k–ω eddy-viscosity model. Their results were compared to experimental data and showed remarkable improvements in the prediction of by-pass transition. Holloway et al. (2004) continued

the development of this approach and presented new results for separated and transitional boundary layers over blunt bodies using also the k–ω model together with the laminar kinetic energy. Cutrone et al. (2007, 2008) used the model of Walters and Leylek (2005) for the prediction of the by-pass and separation-induced transition on flat plates as modeled by the experiments of Coupland and Brierley (1996), which are known as the ERCOFTAC T3A and T3L test cases. In their work, they provided detailed comparisons between a typical intermittency transport approach and the model of Walters and Leylek (2005). The Walters and Leylek (2005) approach provides better results. This is more obvious in the skin friction coefficient plots.

In our work, we proceed one step farther. We attempt to model the separation-induced transition by modeling all the T3L experimental cases using the cubic non-linear eddy-viscosity model developed by Craft et al. (1996) in combination with the laminar kinetic energy concept. Due to its constitutive non-linear expression of the Reynolds-stress, this model has the potential to provide realistic distributions for the Reynolds-stress in the near-wall region, by predicting their anisotropic behavior plus, it models in a more accurate manner the production of turbulence, an issue, which has been proved to be problematic, when a typical linear eddy-viscosity model is used. We choose to model all the six T3L test cases in order to include the cases where the freestream turbulence is extremely low, such as in T3L1, which has $Tu = 0.20\%$, or the air flow has an increased velocity, such as T3L6 where $U_\infty = 10$ m/s. During this investigation, we present additional modifications in order to embody the laminar kinetic energy transport equation into the non-linear eddy-viscosity model and we examine its behavior by comparing its results with the model of Launder and Sharma (1974), the original non-linear model of Craft et al. (1996) and the low-Reynolds number k–ω–*laminar kinetic energy* model of Walters and Leylek (2005). The comparisons are based on the ERCOFTAC database for the measured distributions for both the velocity and longitudinal Reynolds-stress inside the boundary layer.

2. The T3L test cases

The ERCOFTAC collection of the T3L transitional test cases is one of the most detailed collections of experiments regarding the separation-induced transition. The experimental setup (Coupland and Brierley, 1996) is based on the boundary layer development on a flat plate with a semi-circular leading edge with $R = 5$ mm. The Reynolds number of the flow, based on the leading edge radius, is 1603 for the test cases having an inlet freestream velocity equal to 5 m/s, 3205 for the test case having 10 m/s and 801 for the test case with 2.5 m/s. The boundary layer starts as a laminar one, in the flat plate leading edge stagnation point region, and it separates in the horizontal surface of the flat plate. Depending on the freestream conditions, larger and thicker or smaller and thinner recirculation zones occur and thus, different transition durations are measured. Based on Mayle's (1991) work, for the separation-induced transitional cases, transition starts in the middle of the recirculation zone and in most cases continues after the reattachment point.

The measurements have been carried-out using the hot-wire technique and include detailed information for the velocity and longitudinal u-RMS distributions inside the boundary layer, followed by the integral boundary layer parameters and the skin friction coefficient distributions, in order to easily conclude where transition starts and where the boundary layer becomes fully turbulent. Table 1 summarizes the T3L test cases with the freestream conditions corresponding to the longitudinal stagnation point location.

Table 1
T3L test cases: freestream conditions.

Test case	Freestream turbulence intensity at $x = 6$ mm downstream of the flat plate leading edge (%)	Freestream air velocity (m/s)
T3L1	0.20	5
T3L2	0.65	5
T3L3	2.3	5
T3L4	5.5	5
T3L5	2.3	2.5
T3L6	2.3	10

3. Turbulence modeling

3.1. The Launder–Sharma model

The Launder and Sharma (1974) turbulence model has been widely used for the modeling of transitional flows. As a linear model, it has been found that its main disadvantage is the incorrect expression of the production of the turbulence kinetic energy, which is based on the linear Boussinesq's expression of the Reynolds-stresses. This false representation leads to unphysical high levels of turbulence inside the boundary layer starting to develop right after the stagnation point and greatly affects its farther development towards the separation point. On the other hand, the isotropic linear expression of the Reynolds-stresses cannot provide the anisotropic behavior of the Reynolds-stresses in fully developed and turbulent flow regime.

3.2. The cubic non-linear eddy-viscosity model

The model of Craft et al. (1996) was proposed in order to overcome this problem (among other problems regarding the isotropic behavior of the linear models). In this model, the constitutive expression of the Reynolds-stress tensor has a non-linear form and its based on the use of two independent mean tensors, the strain, $S_{ij} = (\partial U_i/\partial x_j - \partial U_j/\partial x_i)$ and vorticity $\Omega_{ij} = (\partial U_i/\partial x_j - \partial U_j/\partial x_i)$ rates:

$$\begin{aligned}\overline{u_i u_j} = {} & \frac{2}{3}k\delta_{ij} - \nu_t S_{ij} + c_1\frac{\nu_t k}{\tilde{\varepsilon}}\left(S_{ik}S_{jk} - 1/3 S_{kl}S_{kl}\delta_{ij}\right) \\ & + c_2\frac{\nu_t k}{\tilde{\varepsilon}}\left(\Omega_{ik}S_{jk} + \Omega_{jk}S_{ik}\right) + c_3\frac{\nu_t k}{\tilde{\varepsilon}}\left(\Omega_{jk}\Omega_{jk} - 1/3\Omega_{kl}\Omega_{kl}\delta_{ij}\right) \\ & + c_4\frac{\nu_t k^2}{\tilde{\varepsilon}}\left(S_{kl}\Omega_{lj} + S_{kj}\Omega_{li}\right)S_{kl} \\ & + c_5\frac{\nu_t k^2}{\tilde{\varepsilon}}\left(\Omega_{il}\Omega_{lm}S_{mj} + S_{il}\Omega_{lm}\Omega_{mj} - 2/3 S_{lm}\Omega_{mn}\Omega_{ml}\delta_{ij}\right) \\ & + c_6\frac{\nu_t k^2}{\tilde{\varepsilon}}S_{ij}S_{kl}S_{kl} + c_1\frac{\nu_t k^2}{\tilde{\varepsilon}}S_{ij}\Omega_{kl}\Omega_{kl} \end{aligned} \quad (1)$$

The expression for the eddy-viscosity incorporates the low-Reynolds effects near the wall and is given by $\nu_t = c_\mu f_\mu k^2/\tilde{\varepsilon}$. Craft et al. (1996) adopted the isotropic dissipation, $\tilde{\varepsilon} = \varepsilon - 2\nu(\partial\sqrt{k}/\partial x_j)$ in order to avoid the use of a wall boundary condition for the ε. In Eq. (1), the coefficients c_i take appropriate values based on model calibration for a number of typical flows. The c_μ coefficient is "strain-sensitized" and is computed from the expression

$$c_\mu = \frac{0.3}{1 + 0.35(\max(\widetilde{S}, \widetilde{\Omega}))^{1.5}}\left(1 - \exp\left[\frac{-0.36}{\exp(-0.75\max(\widetilde{S}, \widetilde{\Omega}))}\right]\right) \quad (2)$$

where the dimensionless strain and vorticity rates are $\widetilde{S} = k/\tilde{\varepsilon}\sqrt{0.5 S_{ij}S_{ij}}$ and $\widetilde{\Omega} = k/\tilde{\varepsilon}\sqrt{0.5\Omega_{ij}\Omega_{ij}}$, respectively. Additionally, the damping function is a function of the turbulent Reynolds number, based on the isotropic dissipation $\tilde{\varepsilon}$, and it is given by the equation:

$$f_\mu = 1 - \exp\left[-(\widetilde{R}_t/90)^{1/2} - (\widetilde{R}_t/400)^2\right] \tag{3}$$

where $\widetilde{R}_t = k^2/\nu\tilde{\varepsilon}$. The transport equation for the turbulence kinetic energy and for the isotropic dissipation rate are given by

$$\frac{Dk}{Dt} = P_k - \varepsilon + \frac{\partial}{\partial x_j}\left[(\nu + \nu_t/\sigma_k)\frac{\partial k}{\partial x_j}\right] \tag{4}$$

$$\frac{D\tilde{\varepsilon}}{Dt} = c_{\varepsilon 1}\frac{\tilde{\varepsilon}}{k}P_k - c_{\varepsilon 2}\frac{\tilde{\varepsilon}^2}{k} + E + Y_c + \frac{\partial}{\partial x_j}\left[(\nu + \nu_t/\sigma_\varepsilon)\frac{\partial \tilde{\varepsilon}}{\partial x_j}\right] \tag{5}$$

The near-wall term E is computed from $E = 0.0022\frac{\widetilde{S}\nu_t k^2}{\varepsilon}\left(\frac{\partial^2 U_i}{\partial x_j \partial x_k}\right)^2$ when $\widetilde{R}_t \le 250$ and the Yap (1987) length scale correction is computed from $Y_c = \max\left(0.83\frac{\tilde{\varepsilon}^2}{k}\left[\frac{k^{1.5}}{2.5\tilde{\varepsilon}y}-1\right]\left[\frac{k^{1.5}}{2.5\tilde{\varepsilon}y}\right]0\right)$.

3.3. The k–ε–k_l and k–ω–k_l models

Both models are based on the use of the laminar kinetic energy concept. In order to present the derivation of the combined nonlinear k–ε model with the laminar kinetic energy transport equation, we describe in details the k–ε–k_l model of Walters and Leylek (2004). This model is a linear eddy-viscosity model, which solves one additional transport equation for the laminar kinetic energy. Its main difference from a typical turbulence model is that it splits the kinetic energy into two parts of energies: the turbulent kinetic energy and the laminar one. These two quantities have different expression for their production but there is one equation for the turbulence dissipation rate, which is connected primarily with the turbulent kinetic energy.

The transport equation for the turbulent kinetic energy is given by:

$$\frac{Dk_T}{Dt} = P_T + R + R_{NAT} - \varepsilon - D_T + \frac{\partial}{\partial x_j}\left[(\nu + \alpha_T/\sigma_k)\frac{\partial k_T}{\partial x_j}\right] \tag{6}$$

Here, P_T is the production of the turbulent kinetic energy and is given by

$$P_T = \nu_{T,S}S^2 \tag{7}$$

an expression which is based on the linear concept of the eddy-viscosity models. For this model, the mean strain and vorticity rate tensors are defined as $S = \sqrt{2S_{ij}S_{ij}}$ and $\Omega = \sqrt{2\Omega_{ij}\Omega_{ij}}$, respectively, with $S_{ij} = 0.5(\partial U_i/\partial x_j + \partial U_j/\partial x_i)$ and $\Omega_{ij} = 0.5(\partial U_i/\partial x_j - \partial U_j/\partial x_i)$. The eddy-viscosity appearing in the production term is the small-scale eddy-viscosity, corresponding to the turbulent flow regime, and it is computed using the typical expression involving a damping function for viscous effects, an effective length scale, the c_μ coefficient plus one more damping function playing the role of an intermittency factor ($f_{\tau,s}$):

$$\nu_{T,s} = f_\nu f_{\tau,s} c_\mu \sqrt{k_{T,s}}\lambda_{eff} \tag{8}$$

where $k_{T,s}$ is the small-scale component of the turbulent kinetic energy corresponding to the non-wall-limited (small scales) energy sections in the near-wall region, computed by

$$k_{T,s} = k_T\left(\frac{\lambda_{eff}}{\lambda_T}\right)^{2/3} \tag{9}$$

with

$$\lambda_{eff} = MIN(C_\lambda d, \lambda_T) \tag{10}$$

where $C_\lambda = 2.495$, d is the minimum distance from the wall and λ_T is the turbulent length scale, $\lambda_T = k_T^{3/2}/\varepsilon$. The c_μ coefficient is strain-sensitized:

$$c_\mu = \frac{1}{A_0 + A_s\left(\frac{Sk_T}{\varepsilon}\right)} \tag{11}$$

with, $A_0 = 4.04$, $A_s = 2.12$, while the damping functions are computed from the expressions:

$$f_\nu = 1 - \exp\left(-\frac{\sqrt{Re_{T,s}}}{A_\nu}\right) \tag{12}$$

$$f_{\tau,s} = 1 - \exp\left[-C_{\tau,s}\left(\frac{\tau_m}{\tau_{T,s}}\right)\right] \tag{13}$$

For these two equations, $Re_{T,s} = k_{T,s}^2/\nu\varepsilon$ is the turbulent Reynolds number for the small turbulence producing scales, $\tau_m = 1/S$ and $\tau_{T,s} = \lambda_{eff}/\sqrt{k_{T,s}}$ are the mean and effective turbulent scales, and the appearing coefficients take the values $A_\nu = 5.5, C_{\tau,s} = 4360$. In Eq. (6), R is a production term modeling the averaged effect of the breakdown of streamwise fluctuations during by-pass transition, and it is computed from the expression:

$$R = C_R\beta_{BP}\frac{k_L}{\tau_T} \tag{14}$$

where τ_T is the effective turbulent time scale, $\tau_T = \frac{\lambda_{eff}}{\sqrt{k_T}}$, β_{BP} is a threshold function, which controls the by-pass transition process,

$$\beta_{BP} = 1 - \exp\left(-\frac{\phi_{BP}}{A_{BP}}\right) \tag{15}$$

$$\phi_{BP} = \max\left[\left(\frac{\sqrt{k_T}d}{\nu} - C_{BP,crit}\right), 0\right] \tag{16}$$

and $A_{BP} = 8$, $C_{BP,\ crit} = 35$.

Again, in Eq. (6), the term R_{NAT} is a production term modeling the natural transition process and is given by:

$$R_{NAT} = C_{R,NAT}\beta_{NAT}k_L S \tag{17}$$

with $C_{R,NAT} = 4$,

$$\beta_{NAT} = 1 - \exp\left[-\frac{\max(\phi_{NAT}^{0.75}\phi_{MIX}^{0.25} - C_{NAT,crit}, 0)}{A_{NAT}}\right],$$

$$\phi_{NAT} = \frac{d^2 S}{\nu}, \quad \phi_{MIX} = \frac{\sqrt{k_L}d}{\nu}$$

a term which is assigned to the mixed transition modes.

The term D_T appearing in Eq. (6) models the near-wall dissipation,

$$D_T = 2\nu\left(\frac{\partial\sqrt{k_T}}{\partial x_j}\right)^2 \tag{18}$$

The turbulent diffusion term in Eq. (6) does not adopt the "eddy-viscosity" turbulence quantity. Instead, it uses an alternative expression for the "turbulent scalar diffusivity", which has a similar form with the typical eddy-viscosity expressions, i.e., it includes the c_μ coefficient and a damping function:

$$\alpha_T = 0.09 f_\nu\sqrt{k_{T,s}}\lambda_{eff} \tag{19}$$

The transport equation for the turbulence dissipation rate is given by:

$$\frac{D\varepsilon}{Dt} = C_{\varepsilon 1}\frac{\varepsilon}{k}(P_T + R_{NAT}) + C_{\varepsilon R}R\frac{\varepsilon}{\sqrt{k_T k_L}} - C_{\varepsilon 2}\frac{\varepsilon^2}{k_T} - \frac{\varepsilon}{k_T}D_T + \frac{\partial}{\partial x_j}\left[\left(\nu + \frac{\alpha_T}{\sigma_\varepsilon}\right)\frac{\partial\varepsilon}{\partial x_j}\right] \tag{20}$$

with

$$C_{\varepsilon 1} = 2\left[1 - \left(\frac{\lambda_{eff}}{\lambda_T}\right)^{4/3}\right] + 1.44\left(\frac{\lambda_{eff}}{\lambda_T}\right)^{4/3},$$

$$C_{\varepsilon R} = 0.21\left(\frac{1.5\lambda_T}{\lambda_{eff}} - 1\right), \quad C_{\varepsilon 2} = 1.92, \quad \sigma_\varepsilon = 1.4$$

The closure of the system of the equations is performed with the inclusion of a transport equation for the laminar kinetic energy:

$$\frac{Dk_L}{Dt} = P_L - R - R_{NAT} - D_L + \frac{\partial}{\partial x_j}\left(\nu\frac{\partial k_L}{\partial x_j}\right) \tag{21}$$

As a first observation, this equation does not use any turbulent scalar diffusivity. The production of laminar kinetic energy is computed with the use of large-scale turbulent viscosity:

$$P_L = \nu_{T,l} S^2 \tag{22}$$

where the large-scale turbulent viscosity is computed from:

$$\nu_{T,l} = f_{\tau,l} C_{11}\left(\frac{\Omega\lambda_{eff}^2}{\nu}\right)\sqrt{k_{T,l}}\lambda_{eff} + \beta_{TS} C_{12}\phi_{NAT} d^2\Omega \tag{23}$$

$$\text{with } f_{\tau,l} = 1 - \exp\left[-C_{\tau,l}\left(\frac{\tau_m}{\tau_{T,l}}\right)^2\right] \tag{24}$$

Additionally, $\tau_{T,l} = \lambda_{eff}/\sqrt{k_{T,l}}$, $\beta_{T,s} = 1 - \exp\left(-\frac{\max(\phi_{NAT} - C_{TS,crit}, 0)^2}{A_{TS}}\right)$, $C_{11} = 3.4\times10^{-6}$, $C_{12} = 6\times10^{-11}$, $C_{\tau,l} = 4360$, $A_{TS} = 2000$ and Ω is the mean vorticity rate.

The laminar kinetic energy uses also a near-wall dissipation:

$$D_L = 2\nu\left(\frac{\partial\sqrt{k_L}}{\partial x_j}\right)^2 \tag{25}$$

Finally, the Boussinesq's expression for the Reynolds-stresses becomes

$$-\overline{u_i u_j} = \nu_{TOT}\left(\frac{\partial U_i}{\partial x_j} + \frac{\partial U_j}{\partial x_i}\right) - \frac{2}{3}k_{TOT}\delta_{ij} \tag{26}$$

where

$$\nu_{TOT} = \nu_{T,s} + \nu_{T,l} \tag{27}$$

and

$$k_{TOT} = k_{T,l} + k_{T,s} + k_L \tag{28}$$

Walters and Leylek (2005) presented also, the k–ω–k_l variance of their original model with some additional modifications in order to enhance the quality of the results. Details of this model can be found in their work.

3.4. The adoption of the laminar kinetic energy concept by the non-linear model

Our work is concentrated to the provision of a non-linear k–ε–k_l model based on the cubic constitutive expression of the Reynolds-stresses proposed by Craft et al. (1996). The effort is primarily focused on Eq. (26), i.e. the formulation of a non-linear expression by using the *total* quantities for the eddy-viscosity and turbulence kinetic energy and on the expressions of the production terms for the turbulent kinetic energy.

The transport equation for the turbulent kinetic energy is:

$$\frac{Dk_T}{Dt} = P_{k,s} + R + R_{NAT} - \varepsilon + \frac{\partial}{\partial x_j}\left[\left(\nu + \frac{\alpha_{T,s}}{\sigma_k}\right)\frac{\partial k_T}{\partial x_j}\right] \tag{29}$$

This equation is based on the original formulation of Craft et al. (1996) for the turbulence kinetic energy transport equation and has two additional production terms, the R and R_{NAT}, taken from the Walters and Leylek (2004) model. Additionally, the turbulent scalar diffusivity $\alpha_{T,s}$ is computed from $\alpha_{T,s} = f_\mu c_\mu \frac{k_{T,s}^2}{\tilde{\varepsilon}_s}$. The production term here is $P_{k,s}$ and is different from the production term P_T appearing in Eq. (6), in order to include the non-linear expression for the Reynolds-stresses. The general form of the production term is given by:

$$P_{k,s} = -\overline{u_i u_j}|_s \frac{\partial U_i}{\partial x_j} \tag{30}$$

Here, the Reynolds-stresses are computed from the non-linear expression presented by Eq. (1) appropriately adapted for the inclusion of the laminar kinetic energy concept, which splits the turbulent properties into small and large-scales. The adapted cubic expression reads:

$$\begin{aligned}\overline{u_i u_j}|_s = {} & \frac{2}{3}k_{T,s}\delta_{ij} - \nu_{T,s}S_{ij} + c_1\frac{\nu_{T,s}k_{T,s}}{\tilde{\varepsilon}_s}\left(S_{ik}S_{jk} - 1/3S_{kl}S_{kl}\delta_{ij}\right)\\ & + c_2\frac{\nu_{T,s}k_{T,s}}{\tilde{\varepsilon}_s}\left(\Omega_{ik}S_{jk} + \Omega_{jk}S_k\right) + c_3\frac{\nu_{T,s}k_{T,s}}{\tilde{\varepsilon}_s}\left(\Omega_{ik}\Omega_{jk} - 1/3\Omega_{kl}\Omega_{kl}\delta_{ij}\right)\\ & + c_4\frac{\nu_{T,s}k_{T,s}^2}{\tilde{\varepsilon}_s^2}\left(S_{kl}\Omega_{ij} + S_{kj}\Omega_{li}\right)S_{kl}\\ & + c_5\frac{\nu_{T,s}k_{T,s}^2}{\tilde{\varepsilon}_s^2}\left(\Omega_{il}\Omega_{lm}S_{mj} + S_{il}\Omega_{lm}\Omega_{mj} - 2/3S_{lm}\Omega_{mn}\Omega_{ml}\delta_{ij}\right)\\ & + c_6\frac{\nu_{T,s}k_{T,s}^2}{\tilde{\varepsilon}_s^2}S_{ij}S_{kl}S_{kl} + c_7\frac{\nu_{T,s}k_{T,s}^2}{\tilde{\varepsilon}_s^2}S_{ij}\Omega_{kl}\Omega_{kl}\end{aligned} \tag{31}$$

Of course, this "small-scale" Reynolds-stress expression does not provide the total Reynolds-stress tensor. Additionally, the quantity $\tilde{\varepsilon}_s$ does not represent a "small-scale turbulence dissipation rate". The theory of Mayle and Schulz (1997) does not involve or define any such property. But, since an expression for the non-linear Reynolds-stresses (which will incorporate all the small scale properties) must be derived in order to compute the production of turbulence, we set a new property for the dissipation

$$\tilde{\varepsilon}_s = k_{T,s}^{3/2}\Big/\lambda_{eff} \tag{32}$$

which is computed from the small-scale turbulent kinetic energy and the effective length scale. Besides, the corresponding term for the production of turbulence provided by Walters and Leylek (2004), Eq. (7), uses the combination of the small-scale turbulent kinetic energy and the effective length scale in a similar manner in order to compute the small-scale eddy-viscosity.

The small-scale eddy-viscosity is computed now, from a similar to Eq. (8) expression:

$$\nu_{T,s} = f_\mu f_{\tau,s} c_\mu \frac{k_{T,S}^2}{\tilde{\varepsilon}_s} \tag{33}$$

Here, the damping function f_μ is the original function of Craft et al. (1996) model. The turbulent Reynolds number needed here is computed using $Re_{T,s} = k_{T,s}^2/\nu\tilde{\varepsilon}$. The damping function $f_{\tau,s}$ is the same with the one used in the original model of Walters and Leylek (2004). It is worth to notice here again, that $\frac{k_{T,s}}{\tilde{\varepsilon}_s} = \frac{\sqrt{k_{T,s}}\lambda_{eff}}{k_{T,s}}$ and $\frac{k_{T,s}^2}{\tilde{\varepsilon}_s} = \sqrt{k_{T,s}}\lambda_{eff}$ an equation, which is consistent with

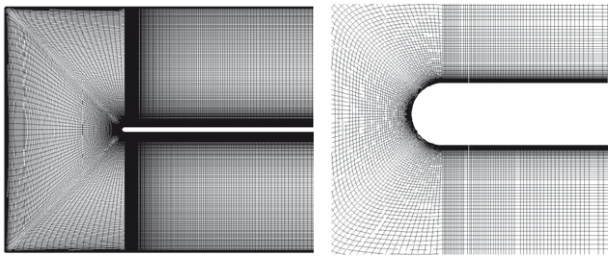

Fig. 1. The O-type grid modeling the computational domain and the flat plate leading edge region.

Eq. (32). For the c_μ function, the expression of the original Craft et al. (1996) model is adopted, Eq. (2). The dimensionless strain and vorticity rates, appearing in Eq. (2), are calculated now using the turbulent kinetic energy and the turbulence dissipation rate.

As an additional comment regarding the turbulence dissipation rate, a close investigation of Eq. (29) shows that the near-wall dissipation term D_T introduced by Walters and Leylek (2004), is included in the Craft et al. Model (1996) when the isotropic dissipation $\tilde{\varepsilon}$ is used since

$$\varepsilon = \tilde{\varepsilon} + 2\nu\left(\frac{\partial\sqrt{k_T}}{\partial x_j}\right)^2 = \tilde{\varepsilon} + D_T \tag{34}$$

The turbulence dissipation rate transport equation reads:

$$\frac{D\tilde{\varepsilon}}{Dt} = C_{\varepsilon 1}\frac{\tilde{\varepsilon}}{k_T}P_{k,s} + C'_{\varepsilon 1}\frac{\tilde{\varepsilon}}{k_T}R_{NAT} + C_{\varepsilon R}R\frac{\tilde{\varepsilon}}{\sqrt{k_T k_L}} - C_{\varepsilon 2}\frac{\tilde{\varepsilon}^2}{k_T} + \frac{\partial}{\partial x_j}\left[(\nu + \frac{\alpha_{T,s}}{\sigma_\varepsilon})\frac{\partial\tilde{\varepsilon}}{\partial x_j}\right] + E + Y_c \tag{35}$$

This equation is the same equation for the dissipation rate provided by Craft et al. (1996) with two additional terms now, modeling the production of turbulence due to natural transition (R_{NAT}) and the rapid reduction of the turbulence length scale during the early stages of transition $\left(C_{\varepsilon_R}\frac{\tilde{\varepsilon}}{\sqrt{k_T k_l}}\right)R$.

Additionally, $C_{\varepsilon 1} = 1.44$, while $C'_{\varepsilon 1} = 2\left[1 - \left(\frac{\lambda_{eff}}{\lambda_T}\right)^{4/3}\right] + 1.44\left(\frac{\lambda_{eff}}{\lambda_T}\right)^{4/3}$, as in the original model of Walters and Leylek (2004).

Finally, the total Reynolds-stresses, as they are used by the momentum equations, are calculated from the expression:

$$\overline{u_i u_j}|_{TOT} = \overline{u_i u_j}|_T + \frac{2}{3}k_L\delta_{ij} \tag{36}$$

where $\overline{u_i u_j}|_T$ is calculated from the constitutive cubic non-linear expression of Craft et al. (1996) using the total eddy-viscosity, Eq. (27) and the turbulent kinetic energy (k_T) together with the turbulence isotropic dissipation rate of turbulence ($\tilde{\varepsilon}$).

4. Computational details

The momentum transport equations, together with the turbulence model equations, are discretized and solved by a vectorized

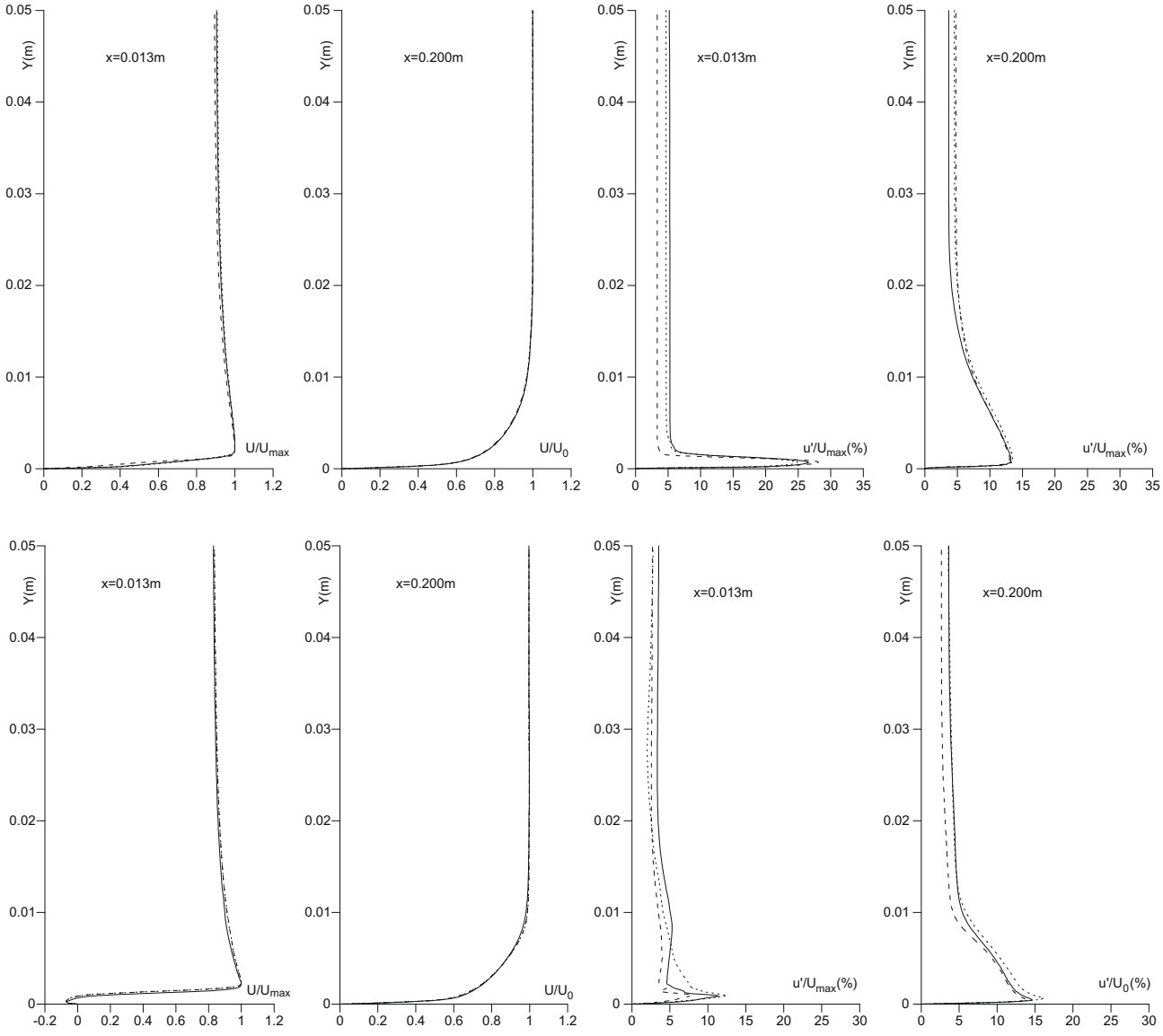

Fig. 2. Velocity and u-RMS distributions for the grid dependency studies. k–ω–k_l model (upper) and NL-k–ε–k_l model (lower). Plain line: basic grid, dashed line: finer grid, dotted line: coarse grid.

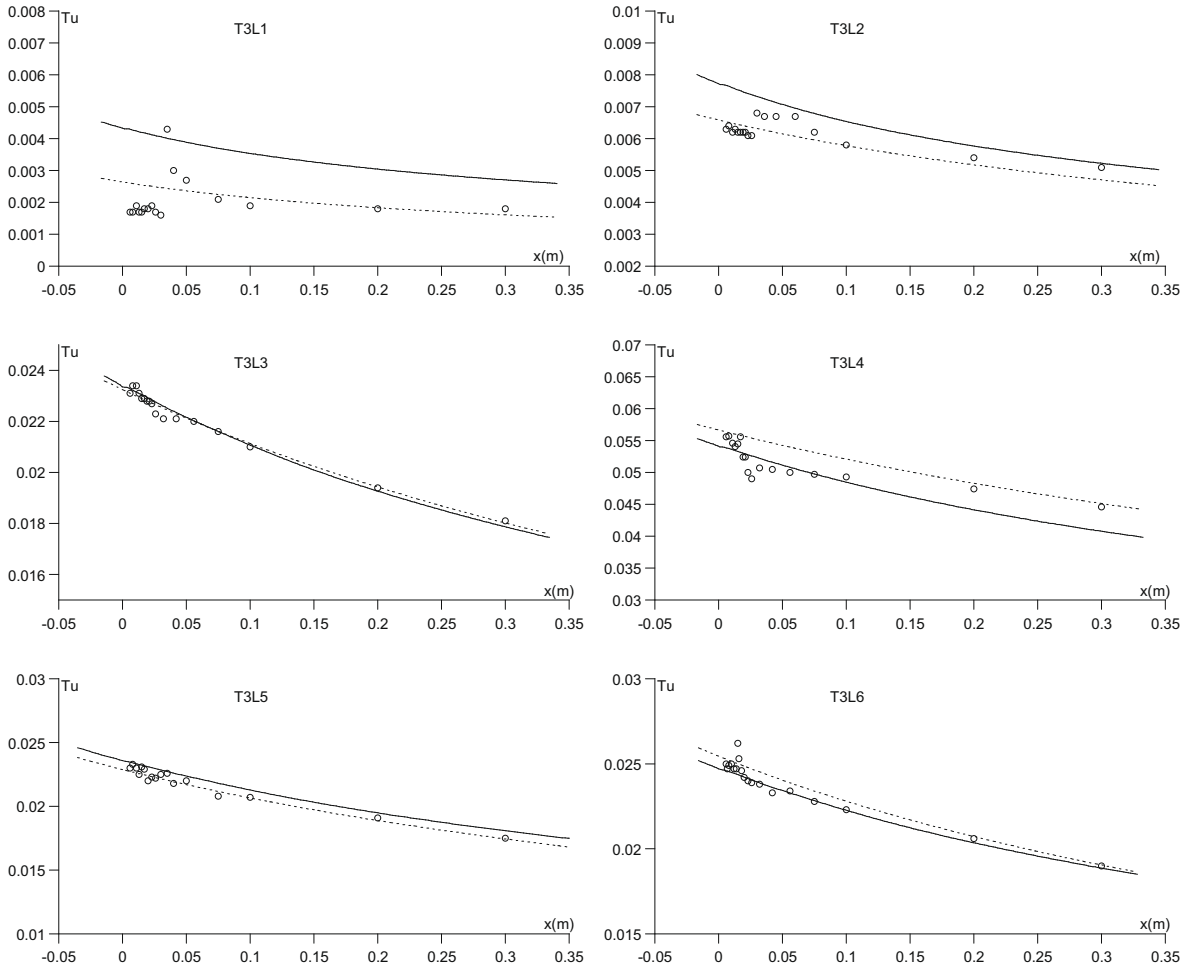

Fig. 3. Freestream turbulence decay. Circles: experiment, plain line: non-linear k–ε–k_l, dashed line k–ω–k_l.

and parallelized solver using a block-structured grid. The numerical scheme of Zhu (1991) is used for the interpolation of the convection and diffusion terms and all the transport equations are solved to a second-order accuracy in order to avoid numerical errors for cases involving transition, as reported by Chen et al. (1998). The grid, Fig. 1, has 114,492 cells, of which, 203 are distributed on the normal to the wall direction and 564 on the flow direction.

Initial runs have been performed in order to check the grid dependency. Three grids have been used, one having half the number of cells and one having the double number, having also the half and the double distances between the cell-centers respectively, except for the cells lying in the near-wall regions. Thus, special care has been taken in order to have y^+ values less than 0.1 for the first computational node adjacent to the wall, while a number of at least 30 cells has been preserved for the calculations inside the boundary layer, for the three grids. The grid dependency studies were focused on the k–ω–k_l model and on the new proposed non-linear (NL) k–ε–k_l model by examining the velocity and longitudinal u-RMS distributions inside the boundary layer. As it can be seen from Fig. 2, both models provided nearly grid-independent results, especially for the two finer grids.

Special care has been also taken in order to have the correct inlet conditions for the turbulent freestream properties, i.e., for the turbulence intensity and the turbulent length scale. Since, the inlet section was located to a certain distance upstream the flat plate, the appropriate turbulence decay has been calibrated (using the experimental data) by using various values for the length scale. This step is inevitable, since an incorrect freestream turbulence decay when an incorrect combination of turbulence intensity and length scale are used can lead to inaccurate predictions, as reported by Vlahostergios et al. (2007) on separation-induced transition modeling using a Reynolds-stress model. Fig. 3 shows the computed freestream turbulence distribution in comparison with the available experimental data for all the test cases. The convergence criterion was set to 10^{-5} for the normalized residuals of the solved variables. Additional measures have been taken into account in order to overcome the unstable behavior of the non-linear model during the iterative procedure, such as manipulating the source terms in the discretized transport equations in order to ensure the dominance of the main diagonal of the tri-diagonal system of equations. It has been found also that when the non-linear model was adopted, a good practice was to start the computations with the linear model and after some preliminary iterations (usually about 100), to switch to the non-linear model. A typical code execution time was about 20 minutes on a small cluster of 22 Apple-G5 CPUs.

5. Results and discussion

The Launder and Sharma low-Reynolds number k–ε model is a good basis to start modeling the flow. A calculation has been performed for the T3L4 case. Fig. 4 shows the predictions for the velocity and longitudinal u-RMS distributions in four selected locations,

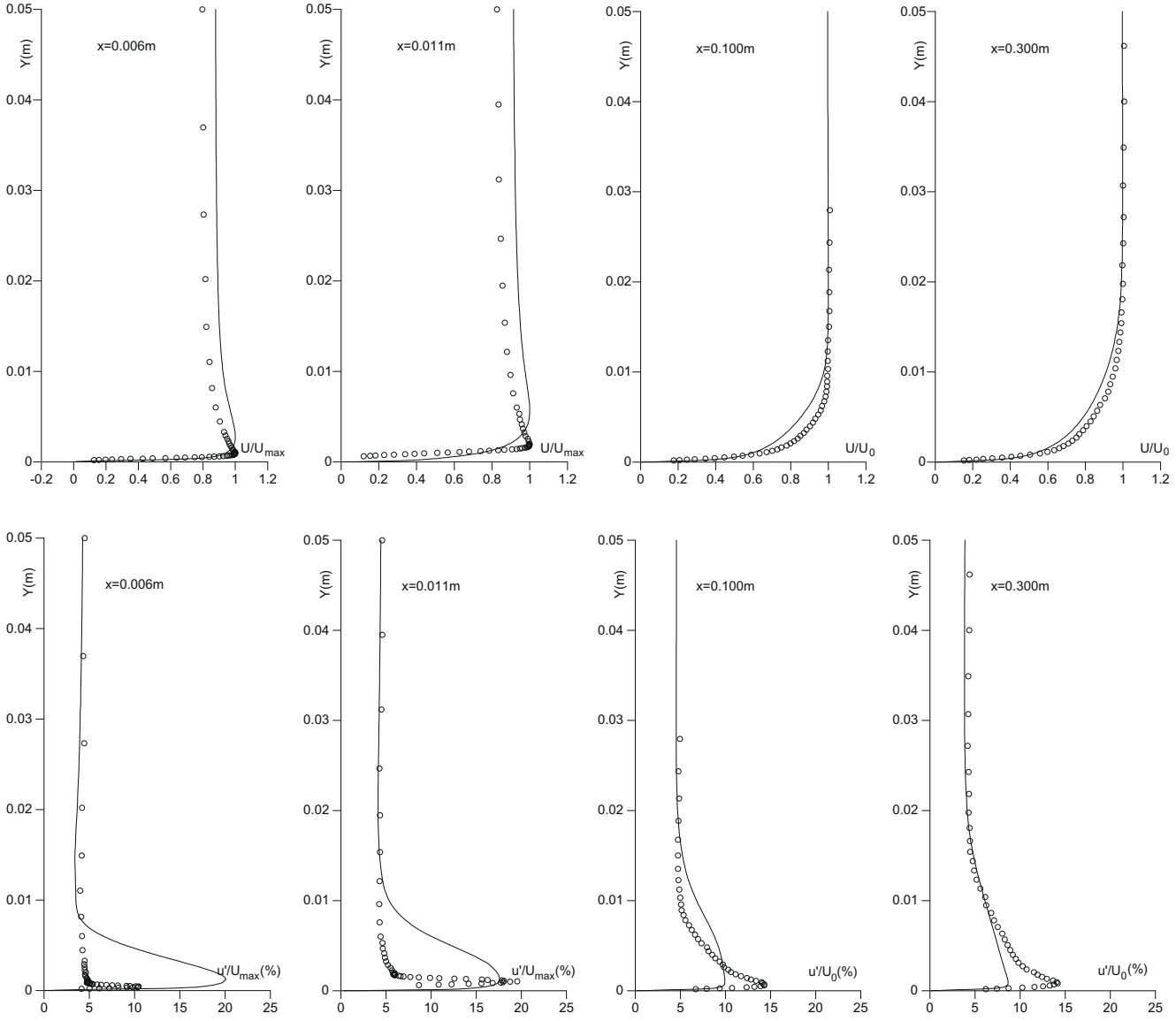

Fig. 4. T3L4: Velocity and longitudinal turbulent fluctuations predicted by the Launder–Sharma model (circles: experiment).

one in the pre-transitional region, where the boundary layer starts to separate, one inside the boundary layer separation and two, downstream the fluid flow and after the boundary layer reattachment point where the flow tends to be fully turbulent.

It is clear that the model underpredicts the recirculation region. As a consequence, transition is not predicted accurately and this is very clearly shown in the far downdtream region (x = 100 and 300 mm) where the velocity distribution of the reattached boundary layer does not fit to the experimental turbulent distribution. Additionally, a closer investigation shows that the laminar boundary layer starts with a larger amount of turbulence (this is clearly shown in the longitudinal u-RMS distributions). This behavior has been attributed in the past, to the false representation of the turbulence production term in the stagnation point region. The use of alternative expressions for the production term, involving the mean vorticity rate tensor (Kato and Launder, 1993), proved to be a good solution for flows where a stagnation point exists, and a laminar boundary layer becomes transitional (Yakinthos and Goulas, 1999). Although the model is very stable, its accuracy is not acceptable. The incapability or the model is depicted also in the shape factor distribution, shown in Fig. 5.

The use of the Craft et al. (1996) non-linear model, in its original formulation was the next step in order to investigate the potential benefits that it could deliver due to the anisotropic expansion of the Reynolds-stresses in the near-wall region and especially near the stagnation point region and inside the transitional flow regime

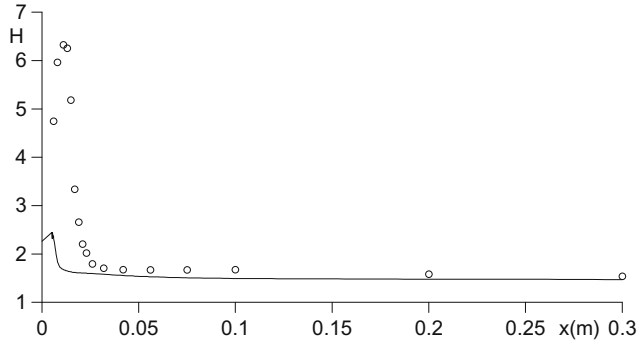

Fig. 5. Boundary-layer shape factor for the T3L4 case, using the Launder–Sharma model.

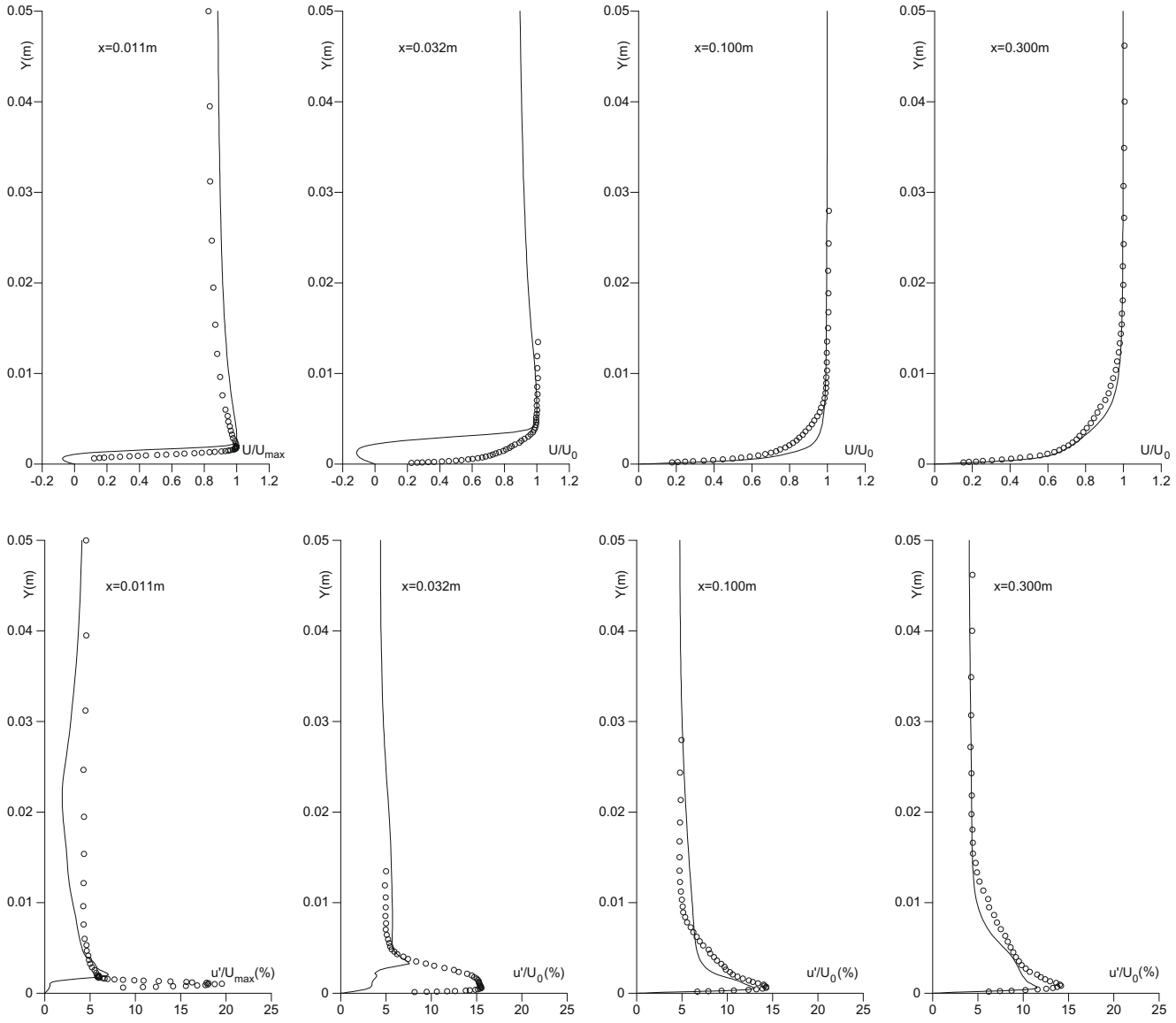

Fig. 6. Predictions obtained using the Craft et al. (1996) model for the T3L4 case.

close to the wall. The T3L4 test case has been selected. The predictions are shown in Fig. 6.

The non-linear eddy-viscosity model is unable to capture the pick values of the longitudinal u-RMS distributions in the pre-transitional flow region. This region is primarily located in the shear layer, close to the recirculation zone interface with the freestream flow. Lardeau et al. (2004) were the first who pointed to this problem for cases where by-pass transition occurs. In order to overcome this problem, they used the concept of the laminar kinetic energy together with the non-linear model of Abe et al. (2003) by incorporating also an intermittency equation for the biasing between the turbulent and non-turbulent eddy-viscosity. Their results showed that indeed, a non-linear eddy-viscosity model with the laminar kinetic energy concept could provide better Reynolds-stress distributions inside the transitional flow regime by predicting in a better way the local maxima in the shear layer. After our tests with the Craft et al. (1996) model we believed that besides the "unphysical" manner of modeling a laminar flow (at the early stages) with a turbulence model, there might be a problem regarding the damping function appearing in the eddy-viscosity expression. It seems that the adopted damping function, overdamps the turbulence and this is surely a combined phenomenon, with the tuned coefficients c_i of the non-linear constitutive expression. Although this expression gives accurate predictions for a fully turbulent profile, for cases where separation-induced transition occurs, the model fails to provide good predictions inside the recirculation region. The computed lower values of turbulence inside the pre-transitional and transitional flow regime, leads to thicker and longer recirculation bubbles, something that is very obvious when one examines the velocity distributions. But, interestingly enough, in the nearly or fully turbulent flow regime, the model provides acceptable results. The overprediction of the recirculation sizes leads to early transition and in the far downstream flow region, where the boundary layer is reattached; the computed velocity distributions present a "more turbulent" nature than the measured ones.

As written previously, the Group of Polytecnico di Bari (Cutrone et al., 2008) presented a detailed study for the application of the k–ω–k_l model to three T3L cases (T3L2, T3L3, and T3L5) together with other models involving also the intermittency transport equation. They concluded that the model of Walters and Leylek (2005) performed the best among the other approaches.

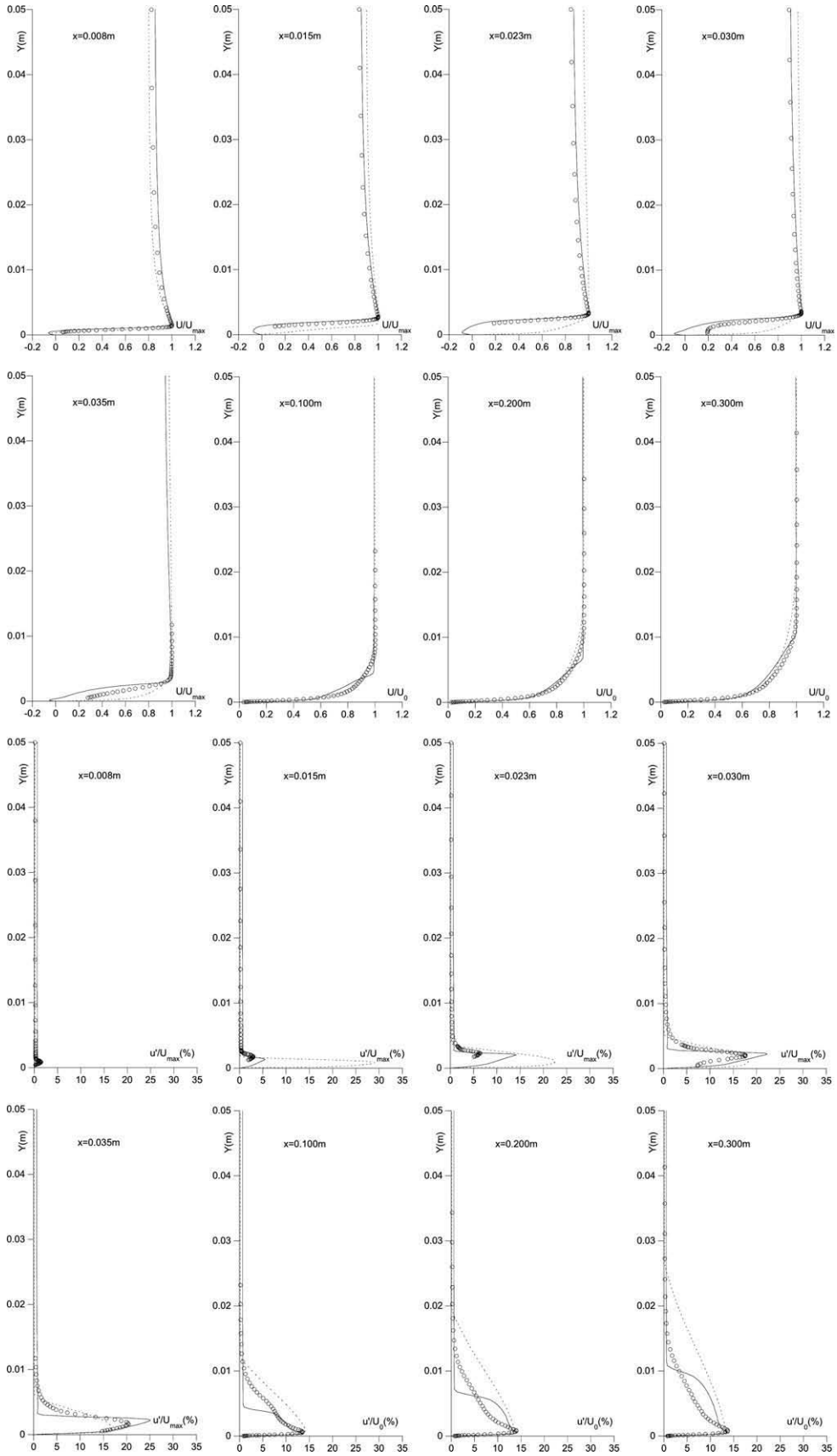

Fig. 7. T3L1. Velocity and longitudinal turbulent fluctuations using k–ω–k_l and NL k–ε–k_l (dashed line: k–ω–k_l, plain line NL k–ε–k_l).

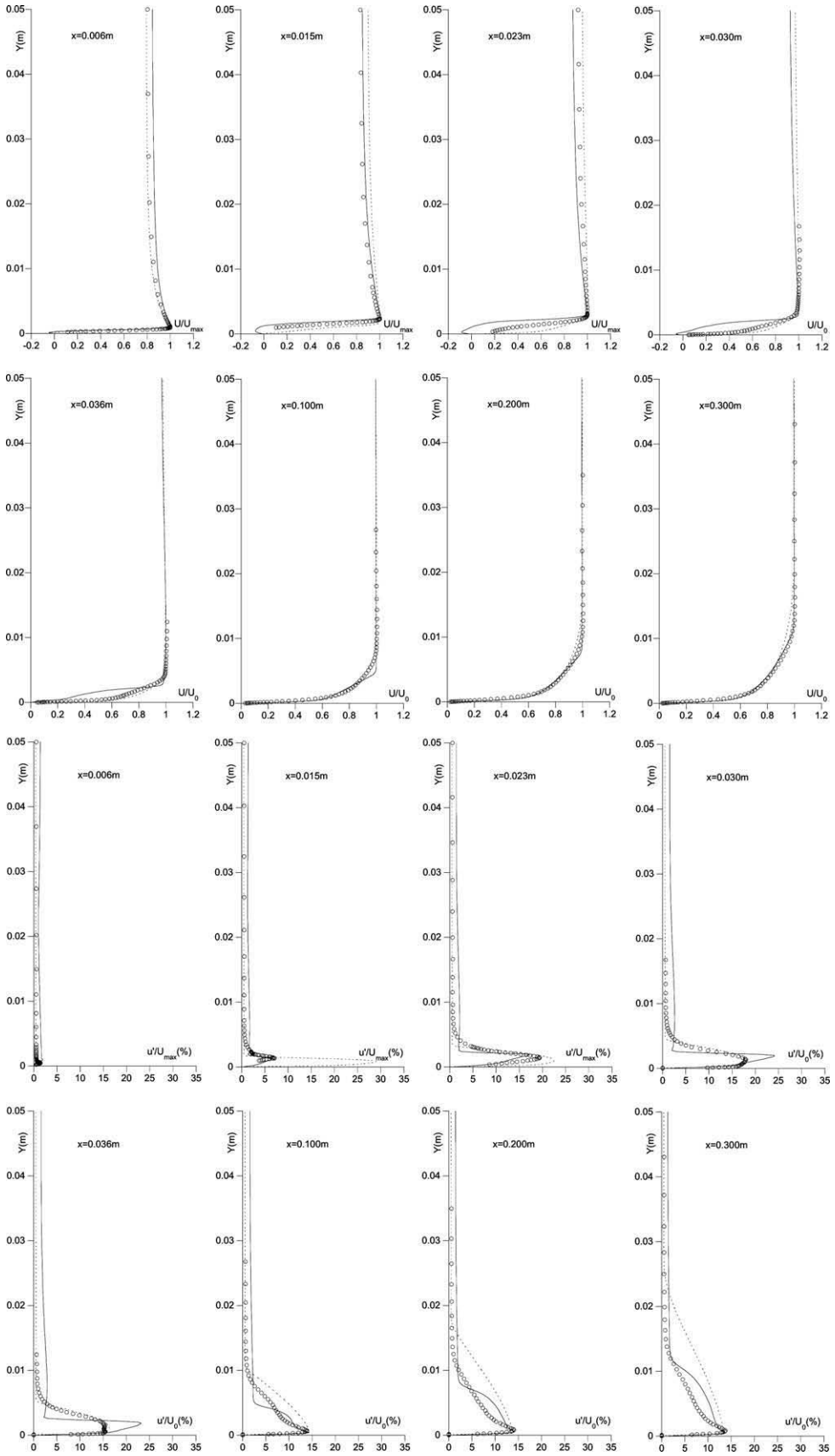

Fig. 8. T3L2. Velocity and longitudinal turbulent fluctuations using k–ω–k_l and NL k–ε–k_l symbols as in Fig. 7.

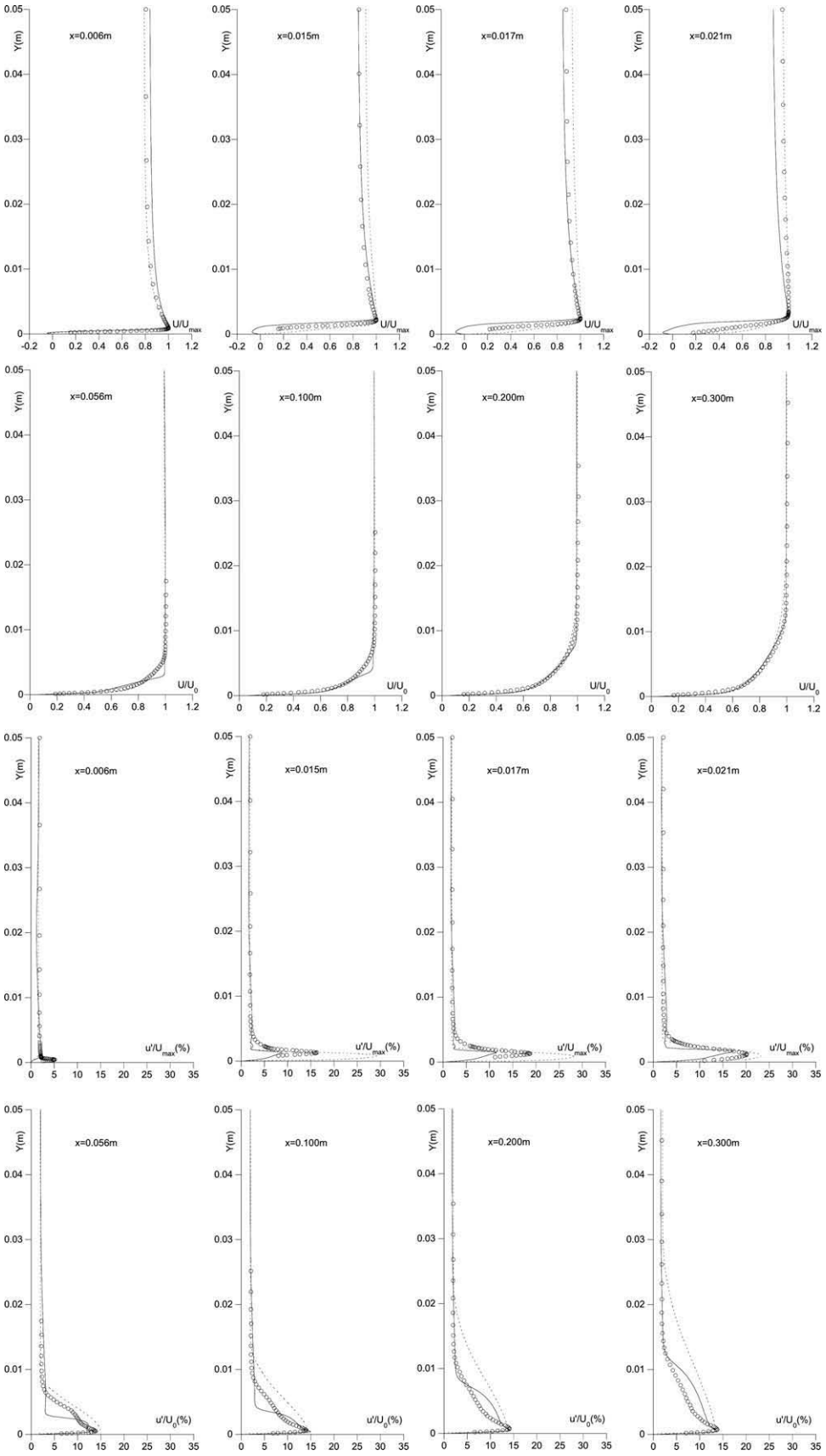

Fig. 9. T3L3. Velocity and longitudinal turbulent fluctuations using k–ω–k_l and NL k–ε–k_l symbols as in Fig. 7.

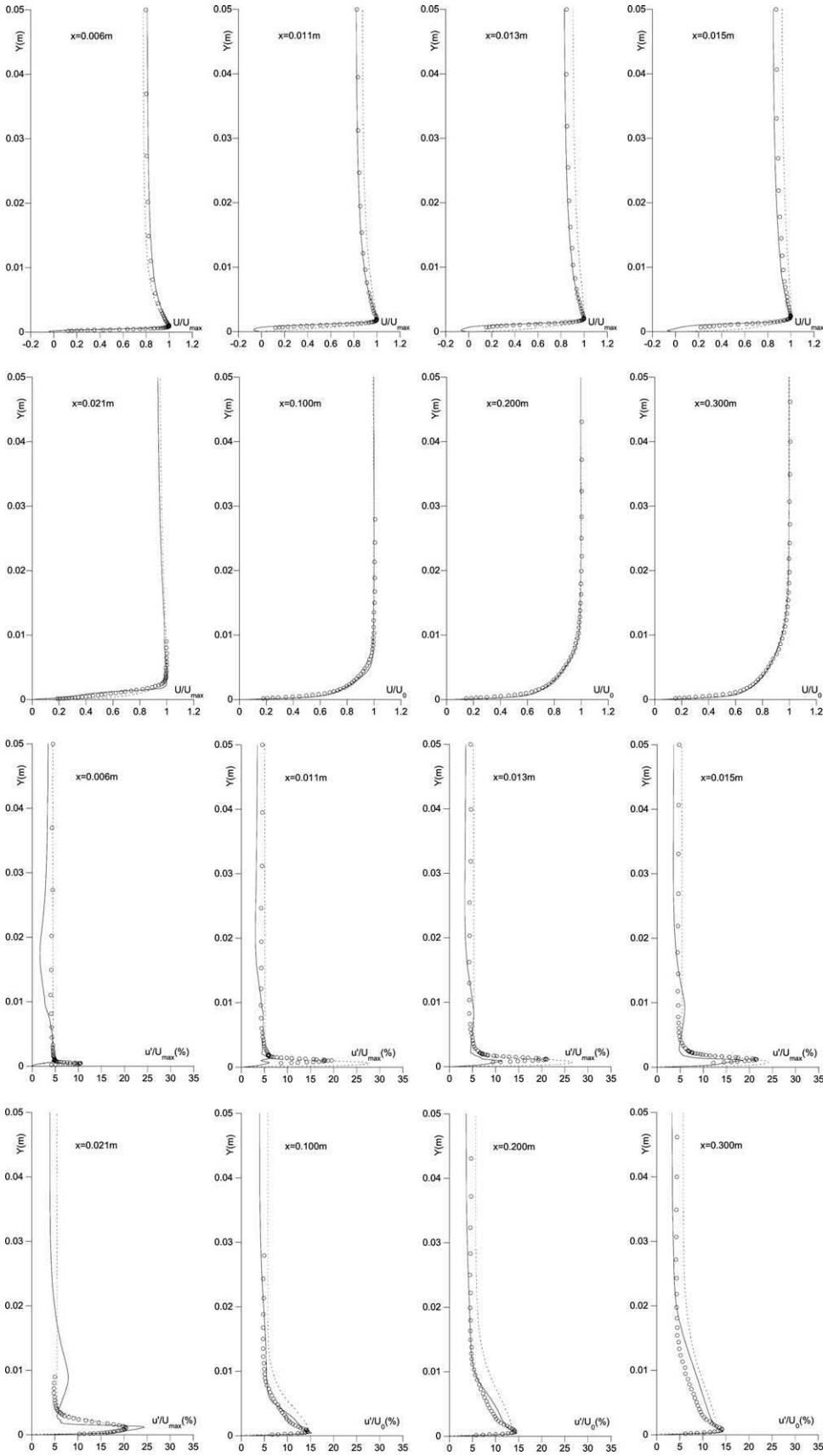

Fig. 10. T3L4. Velocity and longitudinal turbulent fluctuations using k–ω–k_l and NL k–ε–k_l symbols as in Fig. 7.

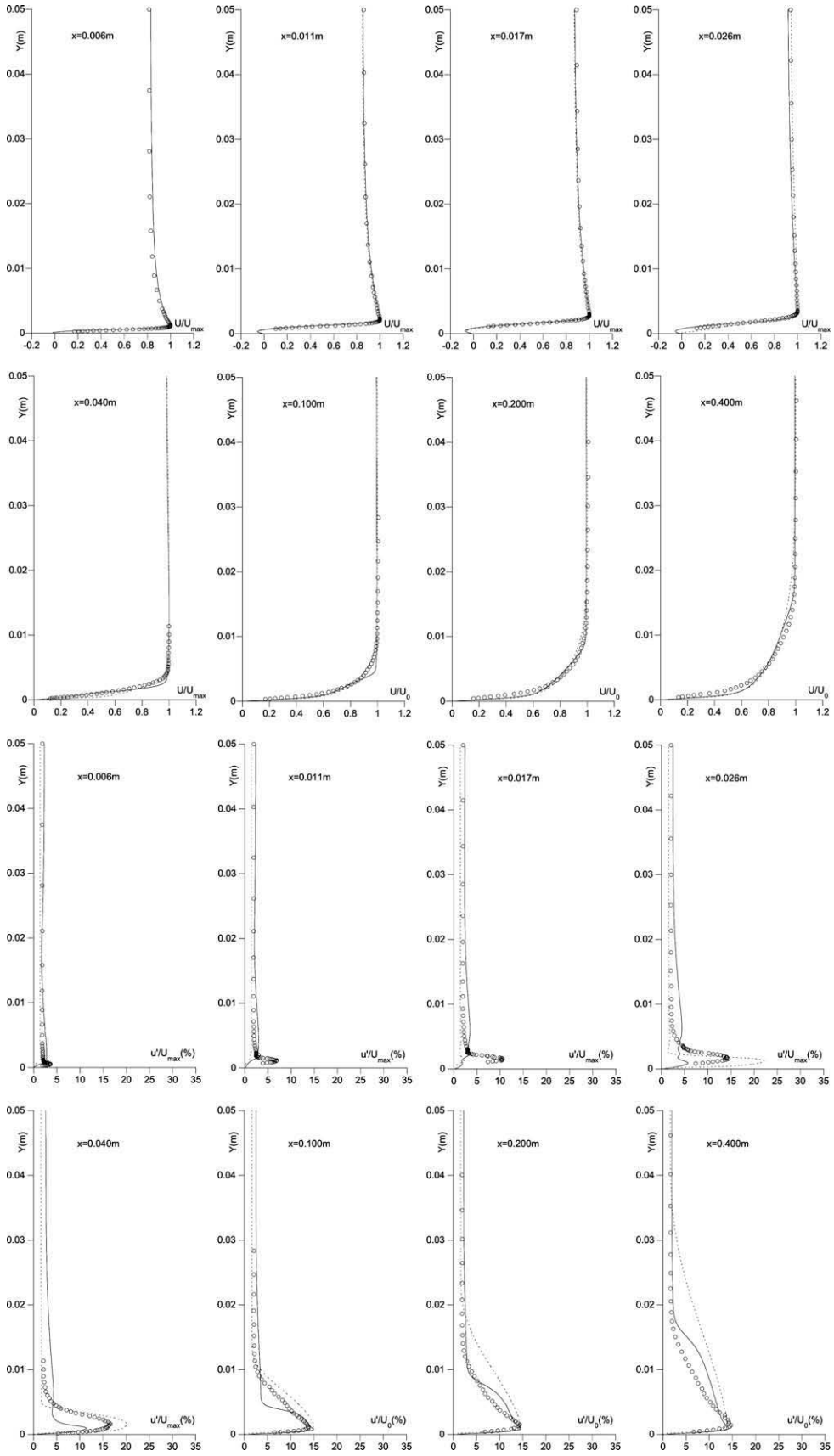

Fig. 11. T3L5. Velocity and longitudinal turbulent fluctuations using k–ω–k_l and NL k–ε–k_l symbols as in Fig. 7.

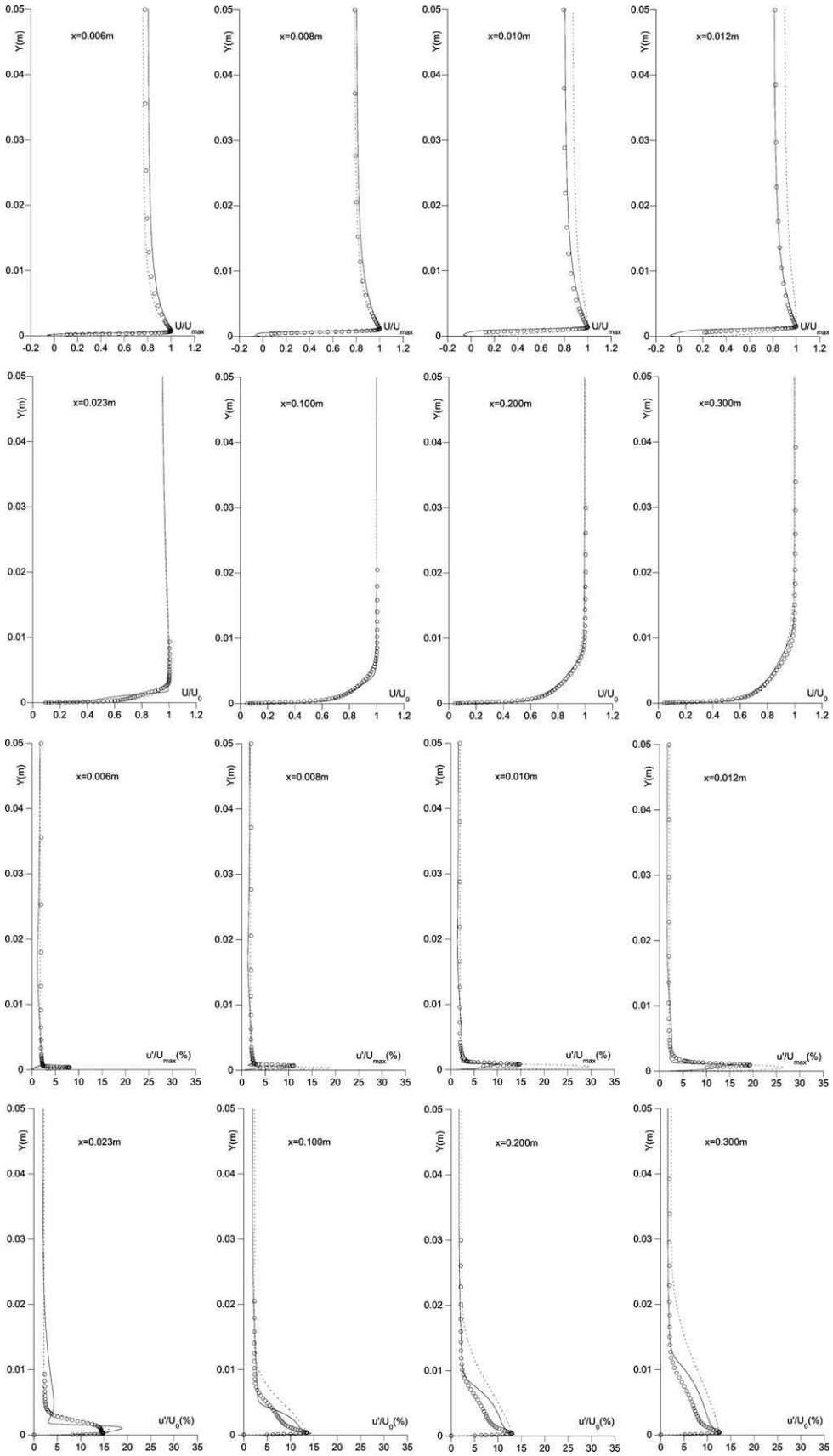

Fig. 12. T3L6. Velocity and longitudinal turbulent fluctuations using k–ω–k_l and NL k–ε–k_l symbols as in Fig. 7.

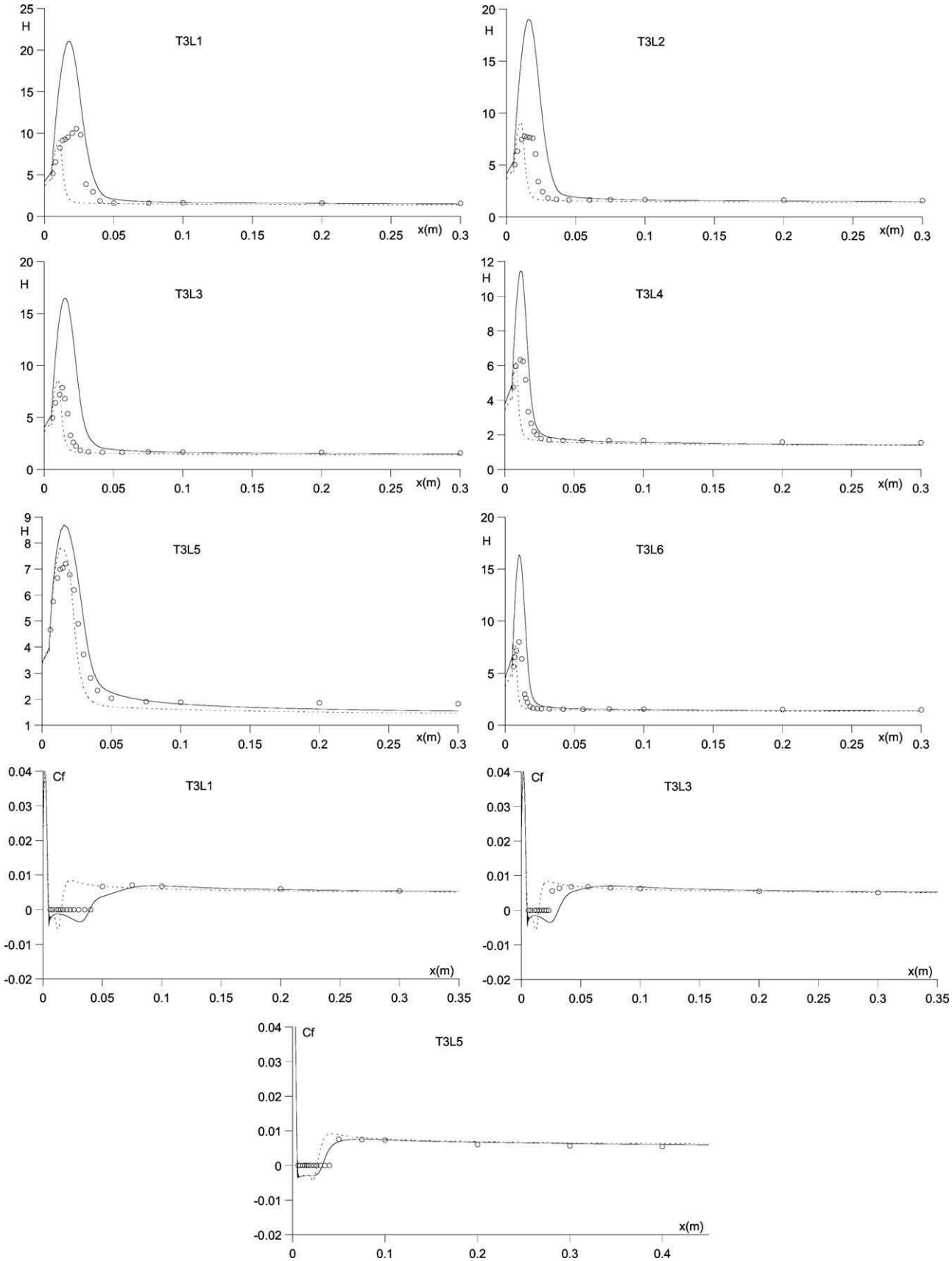

Fig. 13. Shape factor and skin friction coefficient. Symbols as in Fig. 7.

In order to assess the performance of the new combination proposed here, in our final step, we perform a detailed comparison between these two modeling approaches (*linear* k–ω–k_l and *non-linear* k–ε–k_l) by presenting detailed comparisons based on the experimental measurements of velocity and Reynolds-stress distributions.

Figs. 7–12 show the results for the six test cases, using the two models. The comparisons with the experimental data are shown for six locations over the flat plate.

As a general observation, the combined non-linear k–ε–k_l model provides far better results than the original non-linear model of Craft et al. (1996). The predicted velocity distributions are close to the experimental data and the separation zone thickness is more realistically predicted. On the other hand, the k–ω–k_l model shows a remarkable accuracy in some cases, although it tends to predict more turbulent distributions in the pre-transitional locations, something, which is very clear in the cases with low freestream turbulence intensity. For example, when the freestream turbulence has a very low value, as in the T3L1 case, the linear k–ω–k_l model does not predict any boundary layer separation at x = 15 mm and this is closely related to the higher predicted values of the u-RMS shown at x = 15 mm and x = 23 mm. On the same stations, the proposed combination still predicts a separated boundary layer, as measured also in the experiment. This behavior leads to an earlier reattachment location, when the linear model is used, for the separated boundary layer.

The same observations hold for both the T3L2 and T3L3 test cases. Here, again, the k–ω–k_l model presents more turbulent separated boundary layers. The experiments show that the reattachment points for these two cases are located near x = 20 mm for the T3L2 test case and x = 17 mm for the T3L3 test case, but the linear model predicts the reattachment point near x = 15 mm for both cases. Both the velocity and u-RMS distributions show that the linear model overpredicts the amount of turbulence inside the separated boundary layer. On the other hand, for these two test cases, the combined model overpredicts the length and the thickness of the separation zone, although it is able to predict u-RMS distributions closer to the measured ones, especially when the boundary layer is separated.

As an additional comment, for these first three test cases (T3L1, T3L2, and T3L3) the proposed model, fails to correctly predict the smooth distribution measured in the experiment, inside the boundary layer, while the linear model presents an unphysical distribution with much higher values of the u-RMS inside the boundary layer, a behavior which is again closely related to the tendency of the model to overpredict the amount of turbulence inside the boundary layer, when the freestream turbulence is relatively low.

As the freestream turbulence intensity increases, the quality of the results of the linear k–ω–k_l is better, although it tends to overpredict the longitudinal RMS inside the separation zone. For example, in the T3L4 test case and at x = 11, 13, 15 mm, the predicted u-RMS distributions have higher values than the experimental ones. Concerning the T3L5 test case, both models fail to predict correctly the Reynolds-stress distribution inside the recirculation zone.

For the T3L6 test case, the linear model presents, again, a similar behavior, for the majority of the stations shown in Fig. 12. The combined non-linear k–ε–k_l model predicts u-RMS distributions closer to the measured ones, although, in the early stages of transition and especially in the pre-transitional region, (where separation starts), the model fails to capture the peak of the longitudinal RMS distribution. Again, for the T3L6 test case, and concerning the velocity distribution, the combined model tends to overpredict the thickness of the separation zone, while the linear k–ω–k_l model provides clearly a thinner separation zone.

By investigating the u-RMS distributions provided by the combined model, together with the velocity profiles (focusing on the separation zone thickness), it seems that this model has the tendency to increase the damping of turbulence. Probably this is due to the use of the Craft et al. (1996) original f_μ damping function in combination with the strain-sensitized c_μ function. A better calibration of this term could possibly provide better velocity distributions.

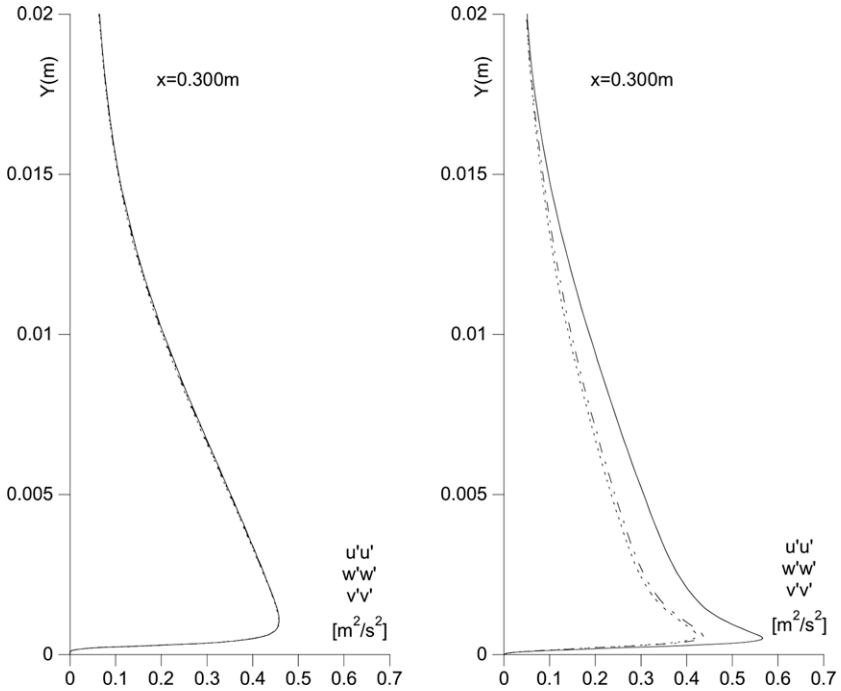

Fig. 14. Near-wall Reynolds-stress distribution. Left: predictions with the k–ω–k_l linear model, right with the new combined k–ε–k_l non-linear model. Plain line: $\overline{u'u'}$, dot-dashed line: $\overline{w'w'}$, dotted line: $\overline{v'v'}$.

Again, we must notice that the combined model provides a specific anomaly in the u-RMS distributions for the far downstream stations, where the boundary layer is attached and becomes fully turbulent. In relation to the T3L1, T3L2 and T3L3 test cases, it seems that this anomaly is more intense for the cases with low freestream turbulence (0.20% and 0.65%). As the freestream turbulence increases, the u-RMS distributions in the turbulent flow regime are more realistic.

The above observations are supported also by the presentation of the boundary layer shape factor development together with the skin friction coefficient (only for the cases where there are available experimental data), for all the examined test cases, shown in Fig. 13.

From the shape factor plots it is clear that the proposed combined model fails to correctly predict the maximum values of the shape factor. This is a major deficit of the model. But, on the other hand, a close observation of the shape factor distributions shows that the proposed model predicts the transition length in a better manner. For example, for the T3L1 test case, despite the incorrect prediction of the peak value, the distribution of the experimental values and the one computed by the proposed model present the same gradients, indicating that the transition length is accurately predicted by the model. The linear model shows clearly, an earlier transition with a shorter length. The superiority of the proposed combined model, for the T3L1 test case, is also shown by the skin friction coefficient distribution. The length of the predicted negative values is the same as the zero values (obviously, the measurement technique is incapable to measure the reverse stresses) length. For the T3L2 test case, the combined model overpredicts again the peak value of the shape factor, but its streamwise location is the same as the one measured in the experiment. The linear $k–\omega–k_l$ model predicts an earlier transition with shorter length. It is very interesting that for the T3L3 test case, the linear model provides far better results, for both shape factor and skin friction coefficient, than the non-linear combined model. It seems that the overprediction of the longitudinal turbulence intensity inside the separated boundary layer (x = 15 mm and 17 mm in Fig. 9) provides a significant contribution to the relatively correct prediction of the transition length. Additionally, the skin friction coefficient predicted by the linear model is of better quality.

For the T3L4, T3L5, and T3L6 test cases, the observations are more or less the same. Again, the combined model predicts longer transition lengths and higher peak values for the shape factor. A closer investigation shows that the streamwise position of the shape factor peak value is correctly predicted by the combined non-linear model, while the linear model predicts an earlier position. In general, the linear model predicts shorter transition lengths and the combined model longer ones.

6. Conclusions

The investigation of the behavior of a new combined turbulence model has been performed in order to assess its capability to predict transitional flows due to boundary layer separation. The new model is based on a cubic non-linear eddy-viscosity model in combination with the laminar kinetic energy concept. The non-linear model in its original formulation, without the use of the laminar kinetic energy, showed that it was totally unable to predict the correct distributions for the u-RMS inside the recirculation region and additionally, provided unphysically large separation regions. In order to overcome this problem, we focused on the correct representation of the Reynolds-stresses by adding the laminar kinetic energy in the pre-transitional flow region. The more accurate representation of the production of turbulent kinetic energy by adopting the non-linear constitutive expression for the Reynolds-stresses has a potential for the provision of more accurate results. The use of the concept of the laminar kinetic energy proved to be very critical since, far better distributions of the u-RMS have been obtained inside the recirculation regions, although some anomalies in these distributions occurred in the fully turbulent flow. It is believed, that a better calibration of the damping function could potentially provide even better predictions with the non-linear eddy-viscosity model. For example, the quality of the results using alternative expressions for the f_μ and c_μ could be investigated. The original model of Walters and Leylek adopts either a strain-sensitized expression for the c_μ or a constant value when it is used for the calculation of the turbulent diffusivity in the k and ω equations. Since the product of f_μ and c_μ must be treated as a compact entity, careful examination of appropriate combinations should be investigated. In this paper, we followed the original concept of Craft et al. (1996) model. In the near future we intend to perform some tests using alternative expressions and we believe that results of better quality can be expected.

In general, the new proposed combined model has been compared with a $k–\omega$ linear model adopting also the laminar kinetic energy. The comparisons between the two models showed that the proposed combined model behaves better in cases where the freestream turbulence intensity is low by predicting in a more correct manner the distributions of the u-RMS inside the separated boundary layer, while it provides satisfactory results regarding the velocity distributions, with a small tendency to overpredict the size of the recirculation zone.

As a final remark, we should refer to the capability of the non-linear model to provide an anisotropic behavior in the near-wall region, as shown in Fig. 14. As reported by Savill (2002a) this is a great advantage of the non-linear models and could perhaps be attributed to the better accounting for the local strain-field effects. Additionally, the non-linear model can handle convex and concave streamline curvature and together with the more accurate modeling of the turbulence production term can improve the predictions on transitional flows.

Aknowledgements

This paper is part of the 03ED360 research project, implemented within the framework of the "Reinforcement Programme of Human Research Manpower" (PENED) and co-financed by National and Community Funds (25% from the Greek Ministry of Development – General Secratariat of Research and Technolgy and 75% from EU – European Social Fund).

References

Abe, K., Jang, Y.-J., Leschziner, M., 2003. An investigation of wall-anisotropy expressions and length-scale for non-linear eddy-viscosity models. Int. J. Heat Fluid Flow 24, 181–198.

Chen, W.L., Lien, F.S., Leschziner, M.A., 1998. Non-linear eddy-viscosity modeling of transitional boundary layers pertinent to turbomachinery aerodynamics. Int. J. Heat Fluid Flow 19, 297–306.

Cho, R., Chung, M.K., 1992. A $k–\varepsilon–\gamma$ equation turbulence model. J. Fluid Mech. 237, 301–322.

Coupland, J., Brierley, D., 1996. Transition in turbomachinery flows. Final Report, BRITE/EURAM Project AERO-CT92-0050. Measurements Available at the ERCOFTAC site.

Craft, T.J., Launder, B.E., Suga, K., 1996. Development and application of a cubic eddy-viscosity model of turbulence. Int. J. Heat Fluid Flow 17, 108–115.

Craft, T.J., Launder, B.E., 1996. A Reynolds-stress closure designed for complex geometries. Int. J. Heat Fluid Flow 94, 245–254.

Craft, T.J., Launder, B.E., Suga, K., 1997. Prediction of turbulent transitional phenomena with a nonlinear eddy-viscosity model. Int. J. Heat Fluid Flow 18, 15–28.

Craft, T.J., 1998. Developments in a low-Reynolds-number second-moment closure and its application to separating and reattaching flows. Int. J. Heat Fluid Flow 19, 541–548.

Cutrone, L., De Palma, P., Pascazio, G., Napolitano, M., 2007. An evaluation of by-pass transition models for turbomachinery flows. Int. J. Heat Fluid Flow 28, 161–177.

Cutrone, L., De Palma, P., Pascazio, G., Napolitano, M., 2008. Predicting transition in two- and three-dimensional separated flows. Int. J. Heat Fluid Flow 29, 504–526.

Durbin, P., Wu, X., 2007. Transition beneath vortical disturbances. Annu. Rev. Fluid. Mech. 39, 107–128.

Gostelow, J., Walker, G., 1991. Similarity behavior in transitional boundary layers over a range of adverse pressure gradients and turbulence levels. ASME J. Turbomach. 113 (4), 617–625.

Hadzic, I., Hanjalic, K., 1999. Separation-induced transition to turbulence. Second-moment closure modeling. Flow Turbul. Combust. 63, 153–173.

Hadzic, I., 1999. Second-moment closure modeling of transitional and unsteady turbulent flows. Ph.D. Thesis, Technische Universiteit Delft.

Hanjalic, K., Jakirlic, S., 1998. Contribution towards the second-moment closure modeling of separating turbulent flows. Comput. Fluid 27, 137–156.

Hazarika, B., Hirsch, Ch., 1992. Transition in turbomachinery flows. BRITE/EURAM Project Contract AERO-0002-C(TT), Report Nr. VUB-STR-19, Final Report.

Holloway, S.D., Walters, K.D., Leylek, J.H., 2004. Prediction of unsteady separated layer over a blunt body for laminar, turbulent and transitional flow. Int. J. Numer. Meth. Fluid 45, 1291–1315.

Kato, M., Launder, B.E., 1993. The modeling of turbulent flow around stationary and vibrating square cylinders. In: Proceedings of the Ninth Symposium on Turbulent Shear Flows, Kyoto, August 1993, pp. 10.4.1–10.4.6.

Lardeau, S., Leschziner, M.A., Li, N., 2004. Modelling by-pass transition with low-Reynolds-number nonlinear eddy-viscosity closure. Flow Turbul. Combust. 73, 49–76.

Launder, B.E., Sharma, B.I., 1974. Application of the energy-dissipation model of turbulence to the calculation of flow near a spinning disc. Lett. Heat Mass Transfer 1, 131–138.

Mayle, R.E., 1991. The role of laminar-turbulent transition in gas turbine engines. ASME J. Turbomach. 113, 509–537.

Mayle, R.E., Schulz, A., 1997. The path to predicting by-pass transition. ASME J. Turbomach. 119, 405–411.

Palikaras, A., Yakinthos, K., Goulas, A., 2002. Transition on a flat plate with a semi-circular leading edge under uniform and positive shear free-stream flow. Int. J. Heat Fluid Flow 23, 455–470.

Palikaras, A., Yakinthos, K., Goulas, A., 2003. The effect of negative shear on the transitional separated flow around a semi-circular leading edge. Int. J. Heat Fluid Flow 24, 421–430.

Savill, A.M., 1995. The Savill–Launder–Younis (SLY) RST intermittency transport model for predicting transition. ERCOFTAC Bull. 24, 37–41.

Savill, A.M., 2002a. By-pass transition using conventional closures. In: Launder, B., Sandham, N. (Eds.), Closure Strategies for Turbulent and Transitional Flows. Cambridge University Press, pp. 464–492.

Savill, A.M., 2002b. New strategies in modeling by-pass transition. In: Launder, B., Sandham, N. (Eds.), Closure Strategies for Turbulent and Transitional Flows. Cambridge University Press, pp. 493–521.

Schlichting, H., Gersten, K., 2000. Boundary Layer Theory, eighth ed. Springer-Verlag, Berlin/Heidelberg/New York.

Schmid, P., 2007. Non-modal stability theory. Annu. Rev. Fluid Mech. 39, 129–162.

Steelant, J., Dick, E., 1996. Modeling of by-pass transition with conditioned Navier–Stokes equations coupled to an intermittency transport equation. Int. J. Numer. Meth. Fluid 23, 193–220.

Suzen, Y.B., Huang, P.G., 1999. Modeling of flow transition using an intermittency transport equation. NASA Report/CR-1999-209313.

Suzen, Y.B., Huang, P.G., Hultgren, L.S., Asphis, D., 2003. Predictions of separated and transitional boundary layers under low-pressure turbine airfoil conditions using an intermittency transport equation. J. Turbomach. 125, 455–464.

Vicedo, J., Vilmin, S., Dawes, W.N., Savill, A.M., 2004. Intermittency transport modeling of separated flow transition. ASME J. Turbomach. 126, 424–431.

Vilmin, S., Hodson, H., Dawes, W., Savill, A., 2002. Predicting wake-passing transition in turbomachinery using an intermittency-conditioned modelling approach. ERCOFTAC Bull. 54, 22–29.

Vlahostergios, Z., Yakinthos, K., Goulas, A., 2007. Experience gained using second-moment closure modeling for transitional flows due to boundary layer separation. Flow Turbul. Combust. 79, 361–387.

Walters, K.D., Leylek, J.H., 2004. A new model for boundary layer transition using a single-point RANS approach. ASME J. Turbomach. 126, 193–201.

Walters, K.D., Leylek, J.H., 2005. Computational fluid dynamics study of wake-induced transition on a compressor-like flat plate. ASME J. Turbomach. 127, 52–63.

Wilcox, D.C., 1991. Alternative to the e^n procedure for predicting boundary-layer transition. AIAA J. 19, 56–64.

Yap, C.J., 1987. Turbulent heat and momentum transfer in recirculating and impinging flows. Ph.D. Thesis, Faculty of Technology, University of Manchester, Manchester, UK.

Yakinthos, K., Goulas, A., 1999. The prediction of flow on a flat plate with a circular leading edge under zero and non-zero pressure gradient. In: I.MECH.E. Third European Conference on Turbomachinery: Fluid Dynamics and Thermodynamics, vol. 1, pp. 135–146.

Zhu, J., 1991. A low diffusive and oscillation free convection scheme. Commun. Appl. Numer. Meth. 7, 58.